https://doi.org/10.5194/acp-2021-314
Preprint. Discussion started: 20 April 2021

Atmospheric Chemistry and Physics Discussions

How weather events modify aerosol particle size distributions in the Amazon boundary layer

Luiz A. T. Machado[1,2], Marco A. Franco[2], Leslie A. Kremper[1], Florian Ditas[1,a], Meinrat O. Andreae[1,3,4], Paulo Artaxo[2], Micael A. Cecchini[2], Bruna A. Holanda[1], Mira L. Pöhlker[1], Ivan Saraiva[5], Stefan Wolff[1], Ulrich Pöschl[1], and Christopher Pöhlker[1]

[1]Multiphase Chemistry Department, Max Planck Institute for Chemistry, Mainz, Germany
[2]Instituto de Física, Universidade de São Paulo, São Paulo, Brazil
[3]Scripps Institution of Oceanography, University of California San Diego, La Jolla, CA 92037, USA
[4]Department of Geology and Geophysics, King Saud University, Riyadh, Saudi Arabia
[5]Sistema de Proteção da Amazônia, Manaus, Brazil
[a]now at: Hessian Agency for Nature Conservation, Environment and Geology, 65203 Wiesbaden, Germany

Correspondence: Luiz A. T. Machado (l.machado@mpic.de)

Abstract. This study evaluates the effect of weather events on the aerosol particle size distribution (PSD) at the Amazon Tall Tower Observatory (ATTO). This research combines in-situ measurements of PSD and remote sensing data of lightning density, brightness temperature, cloud top height, cloud liquid water, and rain rate and vertical velocity. Measurements were obtained by a scanning mobility particle sizers (SMPS), the new generation of GOES satellites (GOES-16), the SIPAM S-band radar, and the LAP 3000 radar wind profiler recently installed at the ATTO-Campina site. The combined data allow exploring changes in PSD due to different meteorological processes. The average diurnal cycle shows a higher abundance of ultrafine particles (N_{UFP}) in the early morning, which is coupled with lower concentrations in Aitken (N_{AIT}) and accumulation (N_{ACC}) mode particles. From the early morning to the middle of the afternoon, an inverse behavior is observed, where N_{UFP} decreases and N_{AIT} and N_{ACC} increase, reflecting a typical particle growth process. Composite figures show an increase of N_{UFP} before, during, and after lightning was detected by the satellite above ATTO. These findings strongly indicate a close relationship between vertical transport and deep convective clouds. Lightning density is connected with a large increase in N_{UFP}, beginning approximately 100 minutes before the maximum lightning density and reaching peak values around 200 minutes later. In addition, the removal of N_{ACC} by convective transport was found. Both the increase in N_{UFP} and the decrease in N_{ACC} appear in parallel with the increasing intensity of lightning activity. The N_{UFP} increases exponentially with the thunderstorm intensity. In contrast, N_{AIT} and N_{ACC} show a different behavior, decreasing from approximately 100 minutes before the maximum lightning activity and reaching a minimum at the time of maximum lightning activity. The effect of cloud top height, cloud liquid water, and rain rate shows the same behavior, but with different patterns among seasons. The convective processes do not occur continually but are modulated by gravity waves in the range of 1 to 5 hours, creating a complex mechanism of interaction with a succession of updrafts and downdrafts, clouds and clear sky situations.

The radar wind profiler measured the vertical distribution of the vertical velocity. These profiles show that downdrafts are mainly located below 10 km, while aircraft observations during the ACRIDICON-CHUVA campaign had shown maximum

https://doi.org/10.5194/acp-2021-314
Preprint. Discussion started: 20 April 2021


Atmospheric Chemistry and Physics Discussions

concentrations of ultrafine particles mainly above 10 km. Our study opens new scientific questions to be evaluated in order to understand the intricate physical and chemical mechanisms involved in the production of new particles in Amazonia.

1 Introduction

The Fifth Assessment Report of the Intergovernmental Panel on Climate Change (AR5 of IPCC, 2013) shows that clouds and aerosols contribute the largest uncertainty in our understanding of the Earth's changing energy budget. Aerosols impact climate, clouds, and precipitation by the direct and indirect effects. Studies based on observations and modeling have improved knowledge and reduced uncertainties regarding the aerosol direct effect (e.g Ramanathan et al., 2001; Hansen et al., 1997); see also Haywood and Boucher (2000) for a review of the estimated direct global annual mean radiative forcing. The effects of natural and anthropogenic sources, such as forest fires and urban pollution, on aerosol-cloud-precipitation interactions, including cloud invigoration as well as precipitation reduction by increased aerosol loading and the associated effects on cloud microphysics have been intensely studied (e.g., Albrecht, 1989; Andreae et al., 2004; Rosenfeld, 2018; Twomey and Warner, 1967; Rosenfeld, 1999; Koren et al., 2005; Rosenfeld et al., 2008; Cecchini et al., 2017a; Heikenfeld et al., 2019). In addition, the knowledge about aerosol characteristics, cloud condensation nuclei (CCN), secondary organic aerosol (SOA) and volatile organic compounds (VOCs) has been greatly improved, specifically in the Amazon region (e.g., Pöschl et al., 2010; Pöhlker et al., 2016, 2018; Palm et al., 2018; Yáñez-Serrano et al., 2020; Holanda et al., 2020; Saturno et al., 2018; Leppla et al., 2021; Schrod et al., 2020). Recently, Artaxo et al. (2021) presented a comprehensive review and discussion of the aerosol effects on climate with a particular focus on tropical and boreal forests. Although these studies have advanced our knowledge of aerosol-cloud interactions, only very few attempts have been made to describe how clouds modify the aerosol properties.

For the Amazon, this topic was recently addressed by two field experiments: Observations and Modeling of the Green Ocean Amazon (GoAmazon2014/5) (Martin et al., 2016, 2017) and ACRIDICON-CHUVA[1] (Wendisch et al., 2016; Cecchini et al., 2017b; Machado et al., 2018). Gerken et al. (2016) discussed the downward transport of ozone by convective clouds and used the surface equivalent potential temperature (θ_e) as a proxy of convective events that produced an increase in ozone concentration at the surface during rainfall events. Wang et al. (2016) analyzed the origin of small aerosol particles in the boundary layer (BL). They found high concentrations of these particles in the free troposphere up to 6 km and concluded that they were transported down by the convective downdrafts during intense precipitation events. Andreae et al. (2018) showed enhanced concentrations of ultrafine particles in the upper troposphere, which were much higher than in the planetary BL. They suggested that these particles were produced in the outflow from deep convective events and were returned to the surface by convective downdrafts. Williamson et al. (2019), using aircraft measurements over the Pacific and Atlantic Oceans

[1] Aerosol, Cloud, Precipitation, and Radiation Interactions and Dynamics of Convective Cloud Systems–Cloud Processes of the Main Precipitation Systems in Brazil: A Contribution to Cloud Resolving Modeling and to the GPM

https://doi.org/10.5194/acp-2021-314
Preprint. Discussion started: 20 April 2021


Atmospheric Chemistry and Physics Discussions

also observed new particle formation in the upper troposphere and suggested that these particles descend towards the lower troposphere, where they can act as CCN, modifying cloud properties.

This study evaluates the effect of weather events on particle number size distribution (PSD) changes, combining satellite and radar data with two scanning mobility particle sizers (SMPS) at 60 and 325 m height at the Amazon Tall Tower Observatory (ATTO) (Andreae et al., 2015). The main cycles and forcings of convective events in Amazonia are evaluated, highlighting the relationship between lightning storms and changes in PSD. This study explores changes in PSD by seasonal and diurnal cycles and the effect of gravity waves, and evaluates the relationships between PSD and lightning, rainfall, cloud top height, cloud liquid water, and brightness temperature during the dry and wet seasons.

2 Data and Methods

This study combines different types of datasets, all colocated at the ATTO site, which is described in detail by Andreae et al. (2015). The data were obtained from the new generation of GOES satellites (GOES-16), the SIPAM S-band radar, two SMPS instruments sampling from 60 and 325 m height above ground and the LAP 3000 radar wind profiler installed at the ATTO-Campina site. ATTO-Campina is a new site to complement ATTO measurements with cloud physics instruments, specifically designed to the study of the aerosol-cloud-precipitation interactions. The Campina site is located about 4 km from the main tower in a small isolated patch, characterized by relatively dry and sandy soils as well as the typical, low Campina vegetation type (Junk et al., 2011). The small size of trees allowed the installation of remote sensing instruments to measure cloud physics. All datasets used in this study were organized and compiled to produce two years of data with 10-minute time resolution, from October 2017 to September 2020. Detailed description of the individual datasets are presented below.

2.1 Scanning Mobility Particle Sizers

This study focuses on particle number size distribution measurements obtained from two Scanning Mobility Particle Sizers (SMPS), which were measuring in parallel at two different sampling heights at the ATTO site. One SMPS was sampling from the 60 m inlet of the triangular mast (TSI Inc., Shoreview, USA; classifiers: first model 3080, later 3082; DMA: 3081; condensation particle counter: CPC 3722) and the second from the 325 m inlet of the Tall Tower (TSI Inc., Shoreview, USA; classifier: 3082; DMA: 3081; condensation particle counter: first 3722, later 3750) (for details, see Andreae et al., 2015; Pöhlker et al., 2016). Both instruments are located in air-conditioned laboratory containers at the foot of the towers. Sample air was transported through stainless steel tubes (finetron tubes, Dockweiler AG, Neustadt-Glewe, Germany) and dried to a relative humidity (RH) below 40 %. At the 60 m inlet, an automatic regenerating silica gel adsorption aerosol dryer, as described in Tuch et al. (2009), was installed upstream of the instruments since 2014 and was replaced by a custom-built and automated condensation aerosol dryer in March 2020. At the 325-m inlet, an automated condensation drier was used since the beginning of measurements. Both SMPS instruments cover a particle size range from 10 to 400 nm, and the sizing accuracy was frequently checked using monodisperse polystyrene latex particles. Data were acquired and exported with the Aerosol Instrument Manager Software (AIM, Version 9 & 10, TSI Inc., Shoreview, USA). The original temporal resolution was 5

https://doi.org/10.5194/acp-2021-314
Preprint. Discussion started: 20 April 2021

Atmospheric Chemistry and Physics Discussions

minutes and was integrated to 10 minutes to maintain the same time resolution as the other data. The data were adjusted for standard temperature (273.15 K) and pressure (1013.25 hPa). The theoretical losses due to the long inlet at 60 m and 325 m were corrected based on a methodology using size-dependent correction factors, as described by von der Weiden et al. (2009).

For the purpose of our analysis, we divided the PSD, obtained by the SMPS over the range from 10 to 400 nm, into the following three individual size classes: (a) ultrafine aerosol particles (UFP) from 10 to 50 nm, (b) Aitken mode particles (AITP) from 50 to 100 nm and (c) accumulation mode particles (ACCP) from 100 to 400 nm (see also multimodal fitting in Pöhlker et al., 2016). In order to evaluate the particle characteristics along the classes, we computed the cross-correlation between the different particles sizes for the Central Amazonian dry (Jun to Oct) and wet (Dec to Apr) seasons. Figure 1 shows how well the multimodal PSDs are described by the aforementioned modes by means of a cross-correlation plot for the dry season. The ACCP and AITP have a clearly defined separation at 100 nm, mainly during the wet season, as this is the location of the Hoppel minimum (Pöhlker et al., 2016). However, the separation among AITP and UFP is not clearly evident. The AITP has a smaller cross-correlation among the particles, which can likely be explained by the fact that this range of particles is in the transition between the other two modes. Specifically, the AITP appears to have sometimes nucleation mode particle properties and sometimes ACCP properties. Clearly, the UFP and ACCP are well cross-correlated among the different particle sizes; however, for the wet season this separation is not well defined. In the wet season there is an increase in cross-correlation from AITP to UFP, but the cross correlation inside the population of the UFP is smaller than during the dry season. The UFP is in a size range where Aitken and nucleation particles modes overlap, therefore we adopted the ultrafine particle denomination for this size range, which showed to be very sensitive and with a different behavior from the other particle classes, as will be shown in this study. Fan et al. (2018) used the same size range to show the effect of UFP in the strengthening of convective updrafts. Given the overlap between the nucleation and Aitken modes and the growth of particles from one mode into the other, the cut at 50 nm is somewhat arbitrary, but as will be shown below, provides a practical basis for discussing the behavior of these particle classes in response to meteorological events and across diurnal and seasonal time scales. Table 1 summarizes the definitions, abbreviations and size ranges of aerosol particle classes used in this study.

Table 1. Definitions, name abbreviations, and symbols of the three aerosol particle size ranges used in this study.

Name of aerosol particle class	**Abbreviation**	**Concentration**	**Diameter (D) range [nm]**
Ultrafine particles	UFP	N_{UFP}	$D \leq 50$
Aitken mode particles	AITP	N_{AIT}	$50 < D \leq 100$
Accumulation mode particles	ACCP	N_{ACC}	$100 < D \leq 400$

2.2 GOES-16

Data from the GOES-16 Advanced Baseline Imager (ABI) channel 13 (10.35 µm) and the Geostationary Lightning Mapper (GLM) were used in this study. The ABI channel 13 has 2 km and the GLM has 8 km spatial resolution, both of them in their original satellite projection. Channel 13 is normally used to estimate the convective cloud depth, where lower brightness

https://doi.org/10.5194/acp-2021-314
Preprint. Discussion started: 20 April 2021

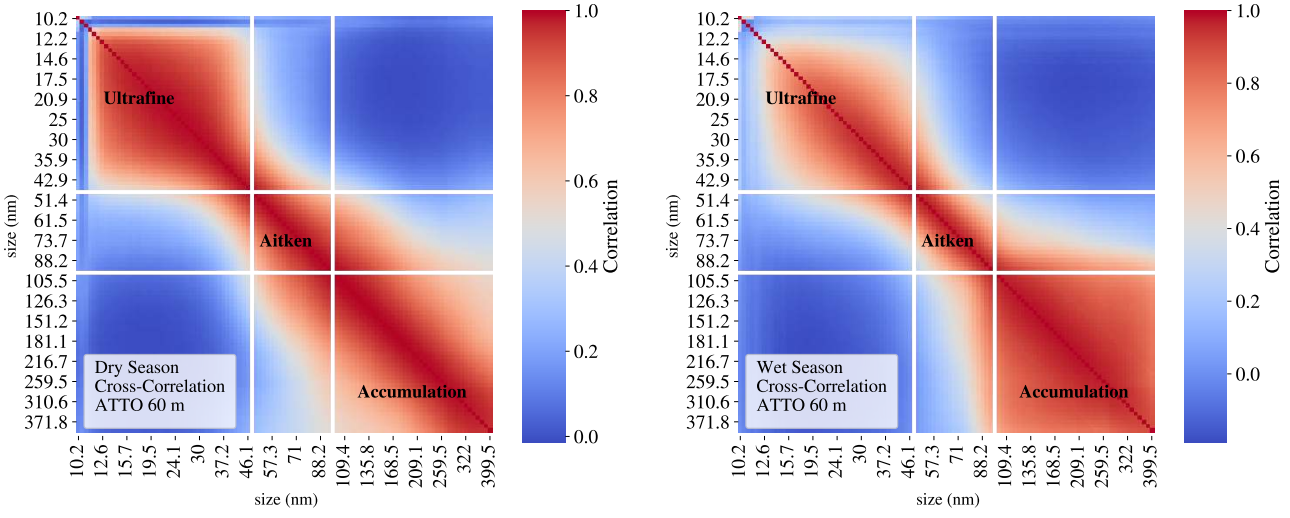

(a) (b)

Figure 1. Particle number size distribution cross-correlation sampled at 60 m height at ATTO. a) Dry season (Jun to Oct) and b) wet season (Dec to Apr). The cross-correlation underlines the distinction into ultrafine, Aitken, and accumulation modes.

temperature (Tir) relates to higher cloud tops simply because the temperature decreases with height in the troposphere (Adler and Mack, 1986). From ABI channel 13, three variables were selected, namely, the ATTO colocated Tir as well as the frequency of occurrence of Tir < 284 K and Tir < 245 K, in a grid of 5 by 5 pixels centered on ATTO. Clear sky radiance in Amazonia is associated with the mixed layer brightness temperature due to the high amount of water vapor near the surface. Machado et al. (2002) used the 284 K threshold to estimate the total cloud cover. The threshold of 245 K is usually employed to describe clouds associated with convective events in tropical regions.

The lightning data were obtained from the GLM, which detects lightning from a 0.74 µm CCD array with a very high temporal resolution, so it can compare the energy peak at different times to define whether it is a lightning or not (detailed description in Goodman et al., 2013). To obtain a better representation of lightning around ATTO, the GLM information was computed as the lightning density: the number of events every ten minutes in an area of 5 by 5 GLM pixels, which corresponds to a description of lightning activity in a 25 km radius.

2.3 S-Band Radar

The SIPAM S-band radar is a weather radar, located in Manaus and operated by SIPAM – (Sistema de Proteção da Amazônia). This S-band radar (10 cm wavelength – 3.0 GHz) has a beam width of 1.8° and a 240 km radius coverage. The radar run

https://doi.org/10.5194/acp-2021-314
Preprint. Discussion started: 20 April 2021


Atmospheric Chemistry and Physics Discussions

occurs every 12 minutes, a volume scan strategy covering 17 elevations. The volume scan produces a 3-D description of the atmosphere. The following parameters were obtained from the 3-D field: The constant altitude plan position indicator (CAPPI) is the reflectivity (dBZ) field at a specific height, in this case we have used the CAPPI at 3 km. There is a direct relationship between reflectivity and rainfall; the Marshall-Palmer relationship considers an exponential drop-size distribution and defines rain rate (R) as: $Z = 200R^{1.6}$, where Z is the reflectivity in ($\mathrm{mm^6\,m^{-3}}$) and R is in $\mathrm{mm\,h^{-1}}$. The CAPPI 3 km is usually associated with the rain rate if rainfall evaporation below 3 km is neglected. The 3 km height is employed to be free of clutter and the Earth curvature effects in the 240 km radius. The echo top corresponds to the maximum height of cloud threshold of 20 dBZ and can be considered as the height of the top of the rain rate associated with the reflectivities describe above. The 20 dBZ echo top is approximately the cloud top of the rain drops (at approximately $1\,\mathrm{mm\,h^{-1}}$). The VIL is the vertically integrated liquid ($\mathrm{kg\,m^{-2}}$). VIL is obtained by the vertical integration of the reflectivity as described by Greene and Clark (1972).

2.4 LAP3000

The LAP3000 radar wind profiler (RWP) is a vertically pointing radar capable of measuring Doppler velocity spectra profiles under both clear sky and precipitation conditions. It operates in the 1290 MHz frequency range, with a 7.1° beam width, and obtains the Doppler spectra based on oscillations of the refractive index of air in the case of clear sky or based on droplet relative motion in the case of precipitation. The instrument is set up to operate in three different modes, one optimized for clear sky and the other two for precipitation. The precipitation modes are obtained in a similar fashion as in Tridon et al. (2013), which aims to convert the RWP to an S-band-like profiler. A similar approach has already been used in the Amazon during the two-year deployment of the Atmospheric Radiation Measurement (ARM) Mobile Facility (AMF) during the GoAmazon2014/5 experiment (Martin et al., 2017, 2016; Giangrande et al., 2017). The present study only used data from one of the precipitation modes, which is able to sample between 1 and 15 km altitude with spatial and temporal resolutions of 210 m and 9.5 s, respectively. The pulse repetition frequency (PRF) is set to 8300 Hz, and the velocity range is between -20 $\mathrm{m\,s^{-1}}$ and +20 $\mathrm{m\,s^{-1}}$ with 0.1 $\mathrm{m\,s^{-1}}$ resolution. The spectra moments are integrated into 5-min intervals for the analysis of the up- and downdrafts.

3 Results and discussion

3.1 Seasonal Cycle

The total particle number concentration varies by about one order of magnitude between wet and dry seasons (Fig. A2 shows the accumulation mode that accounts for most of the particles) (Andreae et al., 2015; Andreae, 2009). Pöhlker et al. (2016) discuss the seasonal variation of cloud condensation nuclei (CCN) in Central Amazonia and conclude that the variability in the CCN concentrations is mostly driven by the aerosol particle number concentration and size distribution. Moran-Zuloaga et al. (2018) present multi-year accumulation and coarse mode measurements at ATTO and discuss the large diversity of the aerosol

https://doi.org/10.5194/acp-2021-314
Preprint. Discussion started: 20 April 2021

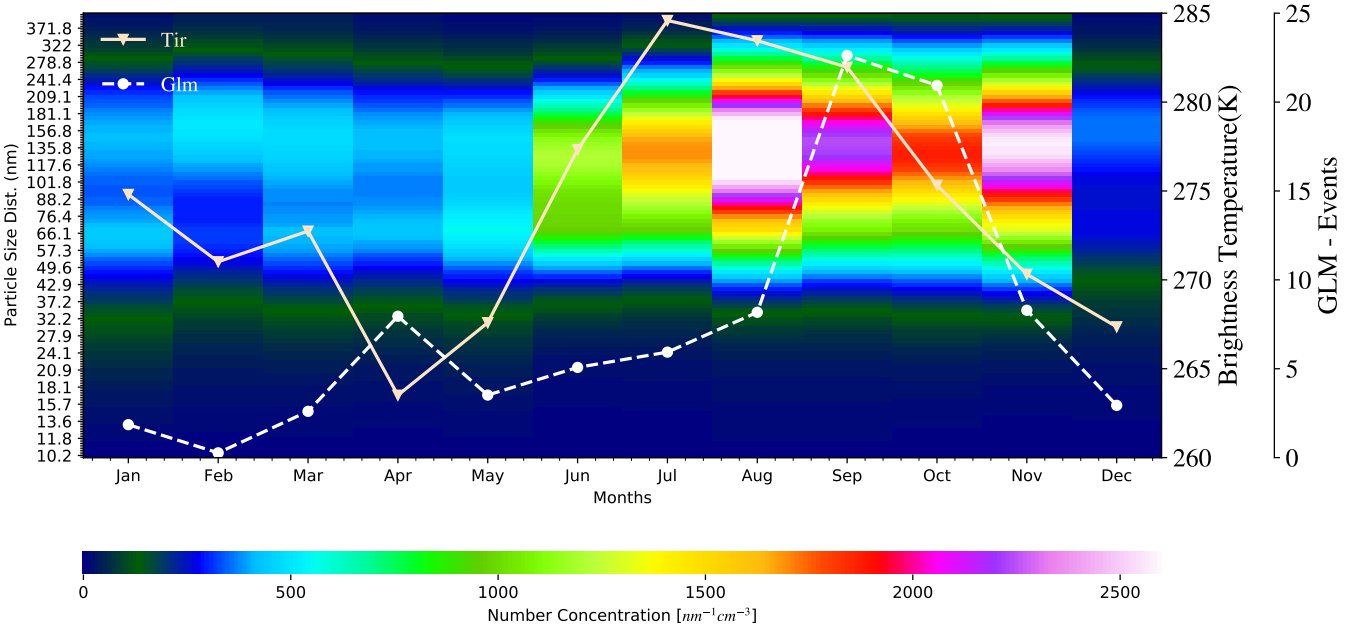

Figure 2. Seasonality of particle size distributions at ATTO (60 m sampling height), brightness temperature (Tir), and GLM lightning density (number of lightnings per 5 minute time bins in area of 50 x 50 km^2 around ATTO). All values are shown as monthly means. Average time frame for all parameters ranges from Oct 2018 to Sep 2020.

sources. (Varanda Rizzo et al., 2018) presents a multi-year analysis of submicrometer particle size spectra at ATTO for wet and dry season. Figure 2 clearly shows this high variability for all sizes, with a maximum number concentration at the end of the dry season, mainly in the range between 100-200 nm.

In addition, Fig. 2 shows the seasonal evolution of the brightness temperature (Tir) and the GLM lightning density. The brightness temperature starts to increase from May to July, characterizing the decrease in cloud cover and in the frequency of occurrence of convective clouds, followed by the increase in particle number concentration. Warm Tir (Tir $>$ 284 K) is associated with low cloud cover or shallow convection and cold Tir (Tir $<$ 235 K) is associated with deep convection. April is the month with the coldest Tir and the rainiest month, but the maximum lightning activity is in September when deep convective rainfall events begin to be more frequent. The brightness temperature and PSD relationship is straight forward, where warmer Tir is associated with reduced rain and high particle concentration and vice versa. However, the lightning activity is highest at the same time that the aerosols have the maximum concentration, indicating that the connection between them is more complex, as will be subsequently discussed in the paper.

The seasonal cycle of the particle number concentration at different altitudes shows interesting features. From the wet to the dry season, the N_{UFP} is nearly constant at 60 m, but increases at 325 m (Figure A1).The absolute value of the difference between the concentration at 60 m and 325 m is small and could depend on the correction employed for losses in the long

https://doi.org/10.5194/acp-2021-314
Preprint. Discussion started: 20 April 2021

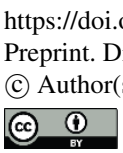

Atmospheric Chemistry and Physics Discussions

inlet tubing at 325 m. The N_{ACC} (Figure A2) has the same phase and nearly the same average concentration at 60 m and 325 m (511 and 556 cm^{-3}, respectively).

3.2 Diurnal Cycle

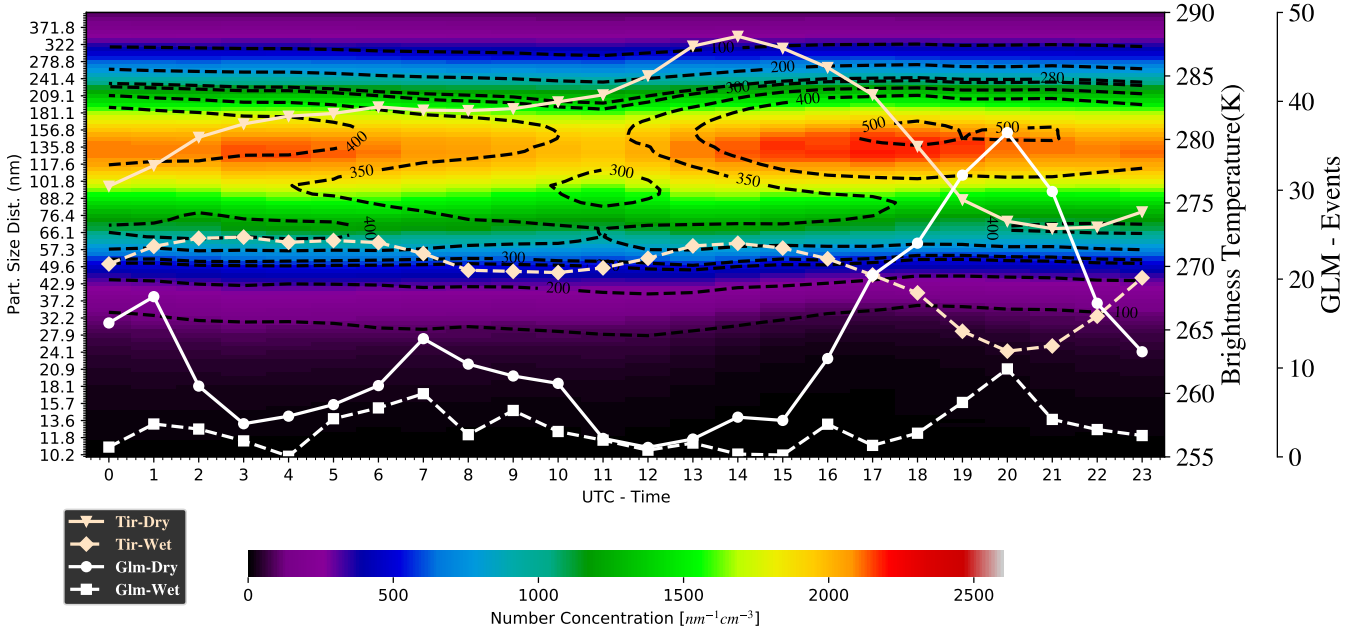

Figure 3. Diurnal cycle of the particle size distribution at ATTO (60 m sampling height) during the dry season (Jun-Oct) in color and wet season (Dec-Apr) as black isolines. The monthly mean brightness temperature and GLM density (number of lighting events in 5 minutes in 50x50 km^2) are plotted as white and gray lines with solid lines for the dry season and dashed lines for the wet season.

Clouds in Amazonia have a typical diurnal cycle during both the wet and dry seasons (Machado et al., 2004). The cloud diurnal cycle as well as BL processes modify the PSD (Betts et al., 2002; Saturno et al., 2018). Figure 3 shows the diurnal cycle of the PSD for the dry (color image) and wet seasons (isolines). Although the dry season has a much larger aerosol concentration than the wet season – on average about factor 5 higher (Moran-Zuloaga et al., 2018) – the diurnal cycle for the wet and dry seasons commonly shows a minimum in N_{ACC} and N_{AIT} at the end of the night and during early morning (i.e., 04:00 to 08:00 local time, which is UTC -4 h). It affects mainly the smaller sizes in the accumulation mode. This minimum during late night and early morning is followed by an increase in N_{ACC} up to the time when Tir starts do decrease and GLM density increases in the afternoon. This is the time when the maximum in N_{ACC} is observed. Moran-Zuloaga et al. (2018) show, for the wet season, that episodic intrusions of African long-range transport of aerosols strongly increase the coarse mode in the early afternoon, when air is mixed down into the PBL from the dust-laden layer aloft.

The increase in the number concentration between morning and noon is coincident with the time when surface sensible heat flux becomes positive, the nocturnal BL is eroded and the convective BL is rapidly built (Stull, 1988; Angevine et al., 2020;

https://doi.org/10.5194/acp-2021-314
Preprint. Discussion started: 20 April 2021

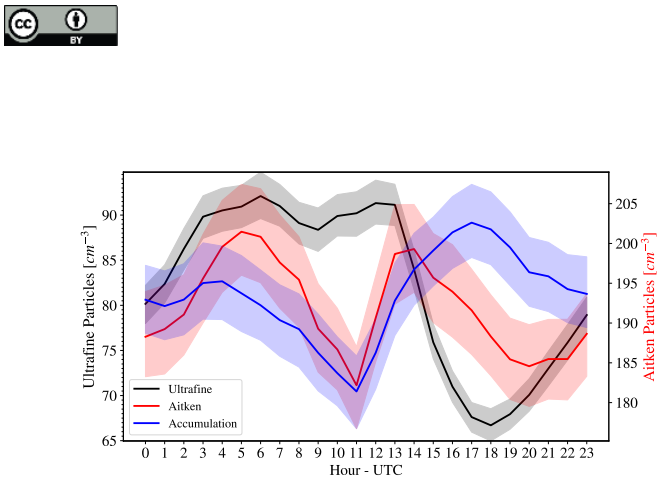

(a)

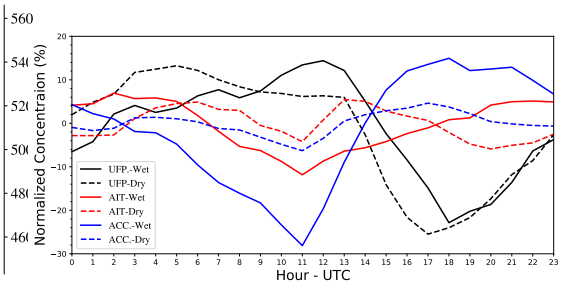

(b)

Figure 4. a) Diurnal cycle of the ultrafine (black), Aitken (red), and accumulation mode particles (blue) at 60 m sampling height. The shaded area corresponds to a confidence interval of 95 %. b) Mean deviation of the diurnal cycle of ultrafine, Aitken, and accumulation mode particles during dry (dashed line) and wet (solid line) seasons.

Fisch et al., 2004). At this time, the BL evolves from the stable stage (nocturnal BL) to the convective BL (mixed layer). Stull (1988) classifies this evolution in four stages: the nocturnal and stable BL stage, the morning transition stage, the rapid growth of the convective BL stage, and the cloudy mixed layer stage. Henkes et al. (2021) show in detail the BL evolution and surface fluxes for these four stages of the development of the convective BL in Central Amazonia during the dry season. The growing stage begins at sunrise and is determined by the time when the surface heat flux passes above zero as well as the turbulent kinetic energy promotes a rapid growth of the convective BL. At this time, the BL exports particles to the free troposphere (the Earth's atmosphere above the planetary BL) and later in the afternoon, they are removed by precipitation scavenging. The differences between wet and dry season convective processes are very clear; from the meteorological point of view, the dry season has higher lightning activity and warmer Tir, and vice versa in the wet season.

To observe the diurnal modulation of PSD in more detail, the daily evolution and relative variation were computed for N_{UFP}, N_{AIT}, and N_{ACC} (Figure 4). N_{ACC} and N_{AIT} decrease during the night; the nocturnal BL height is normally above 60 m (Carneiro and Fisch, 2020), so this decrease is likely related to the interaction between the surface and the BL. This can be attributed to dry deposition to the vegetation and ground surfaces, as there are no other sinks because the exchange across the top of the BL is very small due to the large stability in this layer. Fog could also contribute to this behavior, though the night-time decrease is a systematic behavior during dry and wet season. Whereas N_{ACC} and N_{AIT} decrease during the night, the UFP number concentration remains nearly constant (dry season) or even increases in the wet season. This topic will be specifically discussed in the next section.

This behavior changes completely at sunrise, when accumulation and Aitken particles start to increase and N_{UFP} decreases, with the typical behavior of a particle size growth process, from ultrafine to Aitken and eventually to accumulation sizes (note that N_{AIT} starts to decrease at approximately 13:00 UTC (9:00 LST). This process is observed up to the middle or end of the afternoon, when the concentration of accumulation particles begins to decrease and ultrafine particles increase in phase with the increase in the afternoon convective processes. Figure 4b shows the proportional diurnal variation, relative to the overall

https://doi.org/10.5194/acp-2021-314
Preprint. Discussion started: 20 April 2021


Atmospheric Chemistry and Physics Discussions

mean value, for dry and wet seasons. It is interesting to note that despite their lower concentration relative to the ACCP, the UFP have the largest relative diurnal variation in both seasons. N_{UFP} diurnally changes up to 40 % of the average number concentration. N_{ACC}, as already shown, varies in absolute number much more, but as the number concentration is very high, mainly in the dry season, the relative variation is very small. An exception occurs during the wet season, when N_{ACC} is reduced by up to 30 % during the night. Thus, despite the much larger concentration in the dry season, the relative daily variability is larger during the wet season. This result indicates that the diurnal cycle not only mainly controls N_{UFP}, but also provides a modest decrease in the concentration of the larger modes during the night and shows a growth process from morning to the time that rainfall starts.

The diurnal cycle of N_{UFP} (see Figure A3) has an oscillation in phase among the two heights, with minimal values in the early afternoon. However, the diurnal cycle of N_{ACC} (see Figure A4) shows the number concentration at 60 m having the minimal value earlier than 325 m and a similar concentration in the early morning when the convective BL is developing. This feature shows the importance of the BL evolution in shaping the particle size distribution.

3.3 Weather Events and Particle Size Distributions

This section explores the relationship between lightning/rainfall events and PSD. To understand how the PSD changes as function of the weather events, we evaluate the relationship between thunderstorms (i.e., storms producing lightning) and the evolution of N_{UFP}, N_{AIT} and N_{ACC} from 400 minutes before to 400 minutes after the maximum lightning activity.

To describe the evolution of ultrafine, Aitken and accumulation mode particles, composite analyses were produced based on the maximum GLM density activity. Composite analyses are useful tools to form physical hypotheses on the associations between environmental variables that occur over time (Boschat et al., 2016). Composite analysis is a useful technique to determine basic characteristics of a particular phenomenon. This type of analysis involves collecting large numbers of standardized cases of a given phenomenon and compositing them together as a collection. It involves computing the composite mean and statistical significance of the selected pattern, in this case the lightning occurrence and other cloud characteristics.

The composite depends on the specified threshold to create a collection of cases. For lightning, the threshold was computed as percentiles of the GLM density distribution. This procedure allows comparing different thunderstorm intensities and their effect on PSD, as well as the effect of the other parameters describing cloud activity, such as cloud top height, rainfall, and cloud liquid water. In order to have a comparable selection of lightning intensity and cloud properties, the lightning density selected was defined as a function of the percentile values of 25%, 45%, 65%, 85% and 95%; these percentiles correspond to GLM density events of 2, 30, 137, 494 and 1192 (number of lightning events in 10 minutes in an area of 5 by 5 pixels centered at ATTO), respectively. The composites were produced by selecting the particle number concentration 400 minutes before and after the maximum GLM density for the different values of the selected percentiles. Figure **??** shows the typical evolution of N_{UFP}, N_{AIT}, and N_{ACC} as a function of the maximum GLM density for different percentiles. Figure **??**b also shows the composite of the GLM density for the different percentiles. The number of cases in each composite depends on the percentile and ranges from 2520 for 25% to 159 cases for 95%.

https://doi.org/10.5194/acp-2021-314
Preprint. Discussion started: 20 April 2021


Atmospheric Chemistry and Physics Discussions

At approximately 100 minutes before the maximum lightning density, for any lightning intensity, N_{UFP} particles increase in concentration, reaching maximum values of nearly double the initial concentration 200 minutes later. The difference in N_{UFP} increases exponentially with the GLM percentiles, i.e., the thunderstorm intensity controls the rate of change of the ultrafine number concentration. Deierling and Petersen (2008) found a high correlation between volume updraft and total lightning. Jadhav et al. (1996) showed an increase in ozone (O3) and nitrogen dioxide (NO2) column densities during thunderstorm events. The increase in volume updraft also increases air mass flux and consequently more intense updrafts/downdrafts to the surface, potentially increasing downward advection of ultrafine particles as suggested by Wang et al. (2016) and Andreae et al. (2018). In contrast, N_{AIT} and N_{ACC} decrease, reaching their minimum at nearly the same time as the maximum lightning activity. The main reason for this change could be an exchange of PBL air with air from the free troposphere, which is higher in N_{UFP} and depleted in N_{ACC}, or it cloud be due to the scavenging by the intense rainfall (more efficient for larger particles). These processes will be discussed in the subsection 3.5.

https://doi.org/10.5194/acp-2021-314
Preprint. Discussion started: 20 April 2021

Atmospheric Chemistry and Physics Discussions

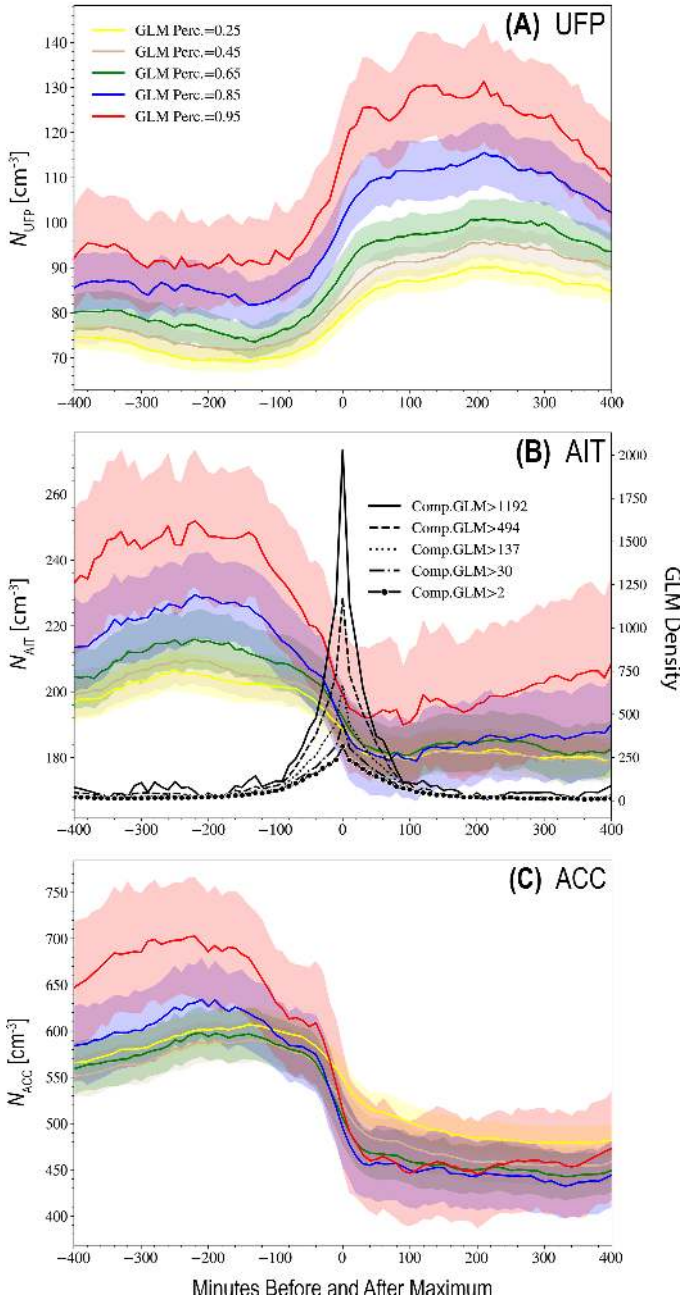

Figure 5. a) Composite N_{UFP} as a function of the maximum GLM density events for different GLM percentiles. b) Composite N_{AIT} as function of the maximum GLM density events for different GLM percentiles. The composite lightning frequency is shown for each percentile from continuous to dashed lines c) Composite N_{ACC} as function of the maximum GLM density events for different GLM percentiles (60 m sampling height). The shaded area corresponds to confidence intervals of 95%.

https://doi.org/10.5194/acp-2021-314
Preprint. Discussion started: 20 April 2021


Atmospheric Chemistry and Physics Discussions

The reason for this increase in concentration of the UFP cannot be answered with the experimental design of this research, but we can hypothesize that the reason is related to them being advected by the convective cloud downdrafts. The results from Wang et al. (2016) and Andreae et al. (2018) suggest that the source of these particles is the upper troposphere, but we will show that the downdraft core is below the source of ultrafine particles in the upper troposphere.

As already mentioned, the changes in N_{AIT} and N_{ACC} happen in an opposite way; these particles are removed, and specifically, N_{ACC} also starts to decrease 100 minutes before the maximum of GLM (the same time N_{UFP} starts to increase). This observation indicates that the rainfall begins at approximately this time and intensifies up to the time of maximum GLM, 100 minutes later. Interestingly, **??** shows that even before the onset of scavenging (i.e., more than 100 minutes prior to the GLM peak), a higher density of lightning is associated with a higher accumulation number concentration. Higher lightning activity appears to be associated with a higher aerosol background condition. The aerosol concentration earlier than 100 minutes before the maximum lightning event is $30\,\%$ higher at the 95th percentile value than that at the 25th percentile. Nonetheless, when approaching the time of maximum lightning activity and even later, the differences in N_{ACC} at the different lightning intensities become equal.

To understand this feedback of higher lightning activity and higher aerosol background, a box-whisker diagram was computed relating GLM density and N_{ACC}, 150 minutes before the maximum lightning event (Fig. 6). This figure highlights the positive correlation between the concentration of ACCP particles several hours before the maximum lightning activity and the increase frequency of the lightning events. This behavior is not clear for all months of the year, although a trend of higher intensity GLM events related to high N_{ACC} is easily observed; however, it is not statistically significant. This lag of 150 minutes before the intense weather event is an average time to detect the aerosol concentration before it is modified by the rain event. During the period from April to August, this relationship is not clearly observed. However, when we look at less polluted months than during the dry season, from December to February (Fig. 6b), this trend is clearer and significant. The reason cannot be answered with the present dataset, but in this period, the effect is better represented than in a highly polluted situation. The sensitivity for invigoration should be higher at low aerosol loadings and become saturated at higher loadings (Rosenfeld et al., 2008). During May and April, the cleanest months (Pöhlker et al., 2018), this relationship is also observed but less pronounced than for the period from December to February. One possible explanation is the very low aerosol particle concentration that reduces the total number of CCN.

https://doi.org/10.5194/acp-2021-314
Preprint. Discussion started: 20 April 2021

Atmospheric Chemistry and Physics Discussions

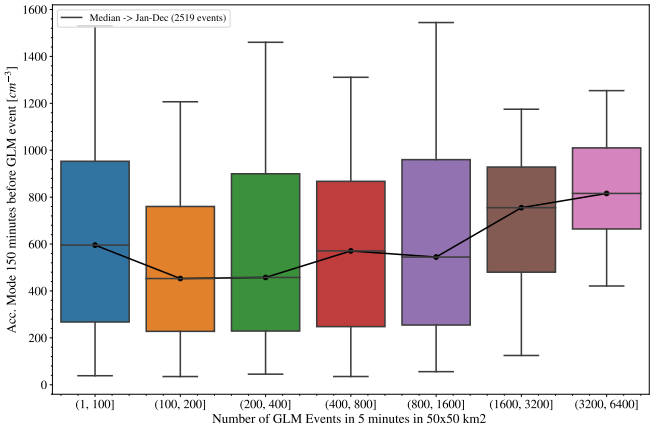

(a)

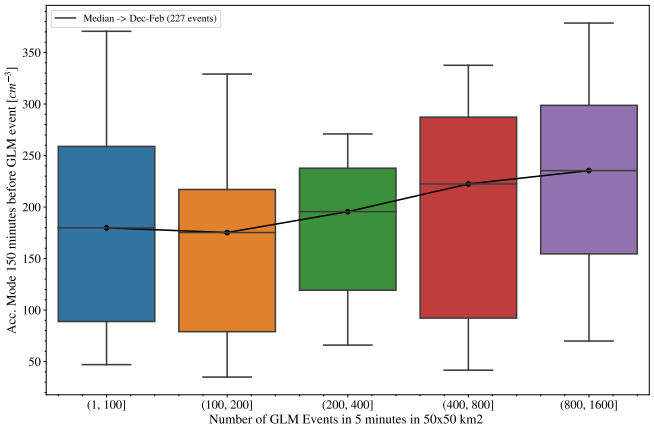

(b)

Figure 6. a) Whisker diagram between GLM density classes and accumulation particle mode number concentration (60 m sampling height), 150 minutes before the maximum lightning density for the two analyzed years. b) The same as (a) but for December to February.

Lightning acting to help increase the concentration of UFP, which hours later grow to accumulation particles and in turn favor more lightning activity is likely related to the convective invigoration processes (Rosenfeld et al. (2008)). This is an interesting behavior, but as we will show, convection is mainly controlled by the convective activity, which is strongly related to gravity waves, and not by the aerosol loading.

For the purpose of analyzing the effect of the rain rate (reflectivity at 3 km), cloud top height, cloud liquid water content, and brightness temperature on the PSD, the same kind of composite figures were prepared. In an effort to combine the different composites in the same figure, the deviations of the means were computed because the absolute magnitudes are different between these weather parameters. The composites are presented only for the maximum event defined by the threshold percentile value of 65 %. For the brightness temperature, since it is a continuous value from clear sky up to deep convective clouds, a

https://doi.org/10.5194/acp-2021-314
Preprint. Discussion started: 20 April 2021


Atmospheric Chemistry and Physics Discussions

selection of the percentile value of $65\,\%$ would be associated with many thousands of values, in contrast to rainfall/lightning events, where the data are only reported for rainfall or thunderstorm (lightning case) events. Therefore the percentiles for Tir were defined only for values smaller than 245 K, normally classified as the clouds associated with convective events (Machado and Rossow, 1993).

Figure 7 presents the evolution of N_{UFP}, N_{AIT}, and N_{ACC} from 400 minutes before to 400 minutes after the maximum of Tir, vertically integrated liquid water (VIL), the 20 dBZ cloud top height (echo top), reflectivity at 3 km (rainfall), and GLM density, respectively, for wet and dry seasons. The results were split into dry and wet seasons due to the different behaviors. The effect on the evolution of particles is similar to the scenario shown for lightning, with a similar phase but with different amplitudes. The larger the amplitude, the more important is the effect of this specific meteorological variable in the modification of aerosol concentration. During the wet season, one can note changes around the mean value on the order of $25\,cm^{-3}$ for the number concentrations from all variables, with the exception of lightning density, which produces larger variations of approximately $40\,cm^{-3}$ in N_{UFP}, N_{AIT} and N_{ACC}. Thunderstorms that produce lightning are more intense than ordinary storms, and this behavior could be explained by the stronger convective updrafts and downdrafts.

The same feature is not observed for the dry season; lightning events are tied to similar or even smaller particle number concentration changes than the other variables. There are some possible reasons for this behavior, such as the large area of 5 by 5 pixels where GLM is observed and the more localized convective cells during the dry season (Machado et al., 2018); this effect could likely minimize the variation of the number concentration at ATTO for smaller systems in the searched region that are farther from ATTO. One interesting point is the similar effect exhibited by the cloud liquid water, cloud top, and rainfall on the evolution of the particle number concentration. These variables are well correlated, but the general effect on particles appears to be mainly related to the rainfall processes and associated updrafts and downdrafts. Recall that GLM captures only lightning that is more intense and closer to the cloud top; therefore, the population of rainfall clouds could also be associated with less intense and shallower lightning events. A second aspect that can be observed in this figure are the different amplitudes of the rainfall effect in the particle number concentration between the wet and dry seasons. For N_{ACC}, for instance, echo top changes imply values of approximately $47\,\mathrm{cm}^{-3}$ in the wet season versus $156\,\mathrm{cm}^{-3}$ in the dry season.

For the purpose of evaluating the rate of change of a specific mode in the particle number concentration (N_{a}) in response to weather events, we select the composite of the GLM and compute the rates of change of the number concentrations for heights of 60 m as well as 325 m. This rate is computed as $\frac{\mathrm{d}Na}{\mathrm{d}t}$ in units of $cm^{-3}\,hour^{-1}$. Figure 8 presents the rate of change of particles in the wet and dry seasons for the GLM composite (maximum threshold percentile value of $65\,\%$). Some noteworthy features can be observed in this Figure. First, UFP concentration changes have nearly the same phase in the wet and dry seasons; they are mainly negative between -400 and -200 minutes and between +200 and +400 minutes and positive between -200 and +200 minutes. The rate of change in the wet season is larger and more than twice that of the dry season value at the time of maximum GLM (minute zero). The rate of change at 60 m is higher than that at 325 m. The ultrafine number concentration increases/decreases in one hour nearly 4 times more at 60 m than at 325 m. This observation indicates that the surface could be the source of the divergence flux of new UFP. Even if the correction for the long inlet at 325 m is not sufficiently accurate to correct the losses of the small particles concentration, this derivative does not depend on the absolute value and therefore

https://doi.org/10.5194/acp-2021-314
Preprint. Discussion started: 20 April 2021

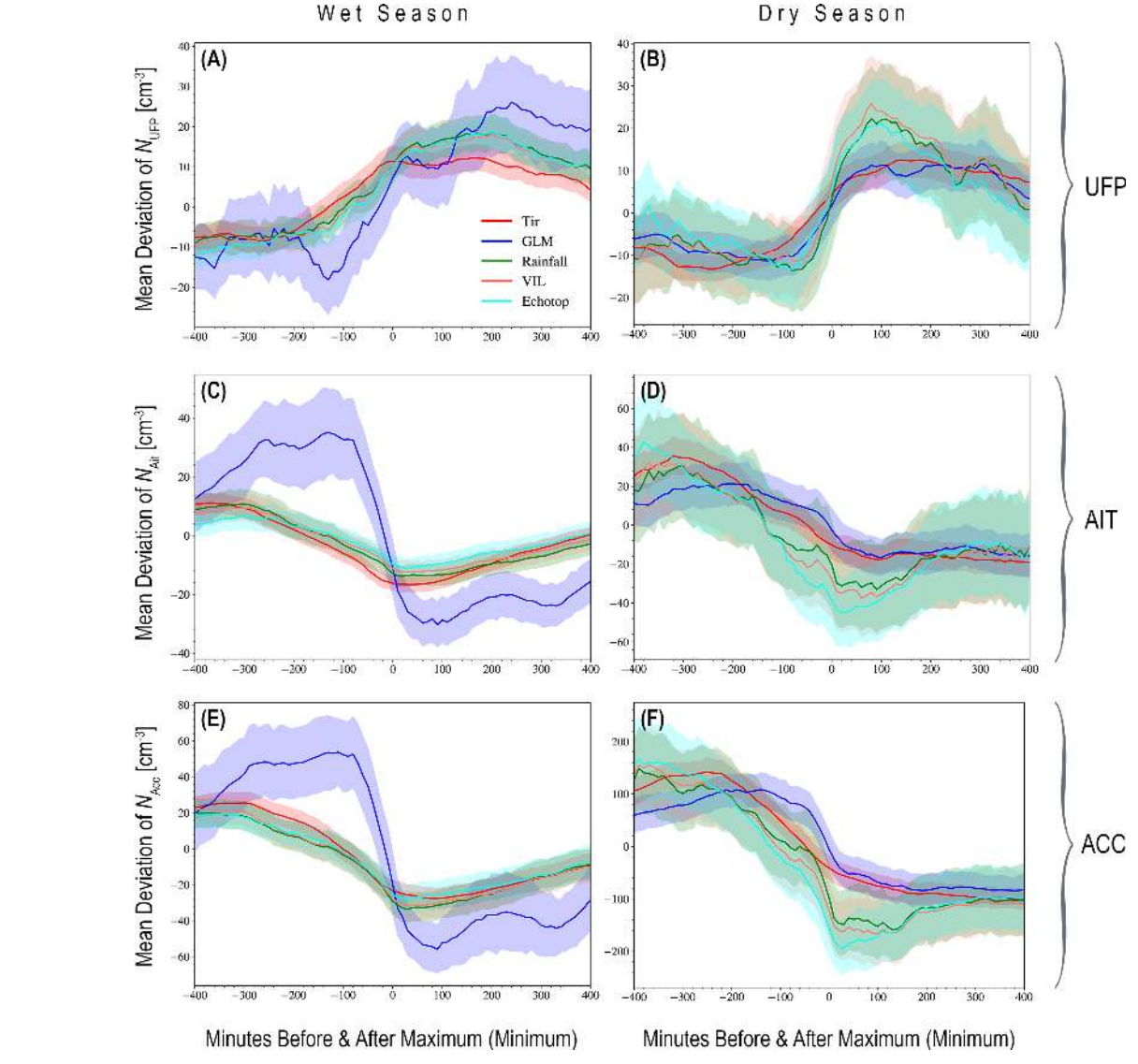

Figure 7. Composite reflectivity, vertically integrated liquid water (VIL), 20 dBZ echo top, brightness temperature, and lightning density for the percentile value of 65 % for a) N_{UFP} during the wet season, b) N_{UFP} during the dry season, c) N_{AIT} for the wet season, d) N_{AIT} for the dry season, e) N_{ACC} for the wet season, and f) N_{ACC} for the dry season (60 m sampling height). The shaded area corresponds to the 95 % confidence interval.

confirms the different behavior between 60 and 325 m. For N_{AIT} and N_{ACC}, in general, between -100 and +100 minutes there is a decrease in concentration and nearly no change during this period, except for N_{ACC} later than +100 minutes, which shows a trend of increased concentration. For the ACCP, the rates of change of the number concentrations at 325 and 60 m have nearly the same magnitude. However, this effect is slightly larger during the dry season at 325 m and during the wet season at 60 m.

https://doi.org/10.5194/acp-2021-314
Preprint. Discussion started: 20 April 2021

Atmospheric Chemistry and Physics Discussions

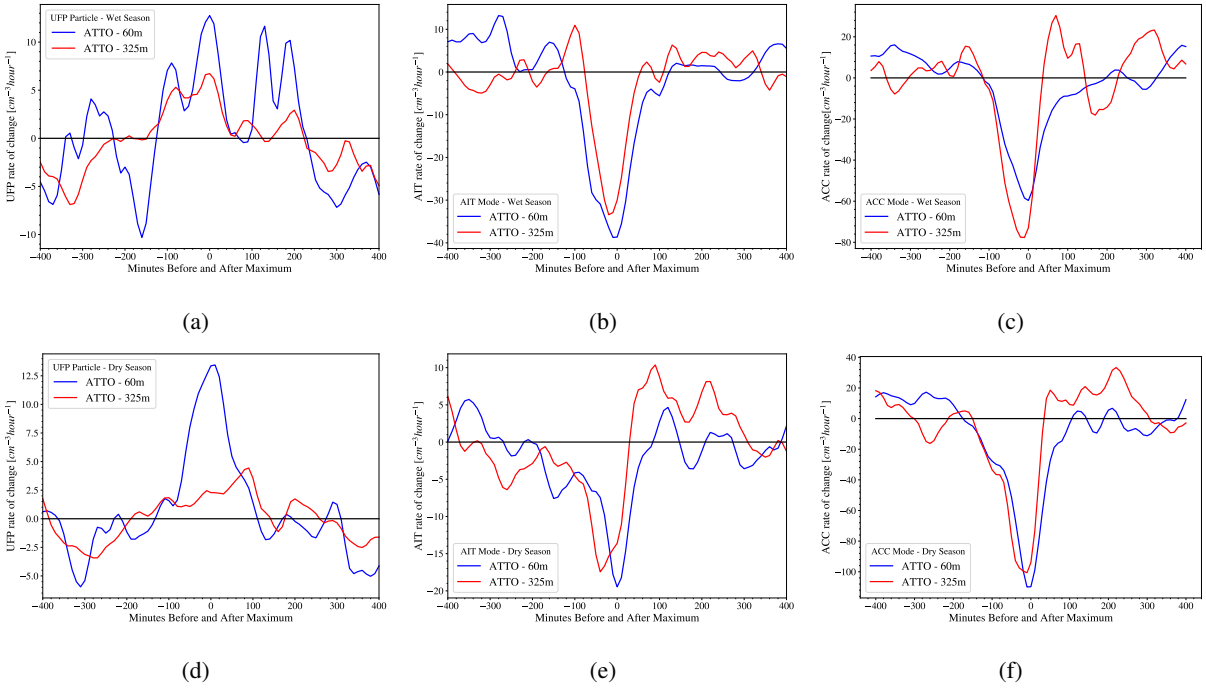

Figure 8. Rate of change in number concentrations from 400 minutes before to 400 minutes after the maximum GLM (0.65 quartile) for a) N_{UFP} at 60 and 325 m during the wet season, b) N_{AIT} at 60 and 325 m during the wet season, c) N_{ACC} at 60 and 325 m during the wet season, d) N_{UFP} at 60 and 325 m during the dry season, e) N_{AIT} at 60 and 325 m during the dry season, and f) N_{ACC} at 60 and 325 m during the dry season

The rate of change also decreases with height. It is possible that at the time when the convective BL is being built, the UFP are advected to higher levels. When the sun rises, N_{UFP} decreases, likely by the growth into the AITP range, reducing N_{UFP} in the BL where the concentration of the AITP and ACCP is higher than that in the free troposphere (Schulz et al., 2018).

Another interesting feature is the high variability of the rate of change of particle concentrations. It is clear that the variability is in the frequency of hours, indicating pulses of increase/decrease in the rate of change in the number concentration. In the next section, we will explore the gravity wave variability that strongly controls the convective cloud modulation as well as the downdrafts and updrafts.

3.4 Gravity waves

Deep convection produces gravity waves that control the variability of convective clouds (Lane and Zhang, 2011). Vertical gravity waves produced by convective towers have an important effect on cloud variability (Alexander et al., 1995). Strong updrafts induce tropopause fluctuations that are spread throughout the troposphere, and latent heat release due to convection and interactions with the mean flow produce gravity waves (Grimsdell et al., 2010). Wang (2007) observed plume formation above thunderstorm anvils, and in simulating this case, they observed high instability and breaking of the gravity waves excited

https://doi.org/10.5194/acp-2021-314
Preprint. Discussion started: 20 April 2021

Atmospheric Chemistry and Physics Discussions

by the strong convection inside the storm. Using the day/night band from the Suomi National Polar-orbiting Partnership (NPP) satellite, Miller et al. (2015) shows several examples of thunderstorms triggering a broad spectrum of gravity waves.

To evaluate the gravity waves, wavelet transforms were employed to compute the time series of the amplitude of the frequencies in intervals with a range of 1-5 hours. The Morlet wavelet was applied to a frequency of Tir < 284 K, to account for the variability of the total cloud cover. The variability in the interval of 1-5 hours was integrated and produced a 10-minute time series; the higher values of this time series were used as a proxy of high gravity wave activity in the interval of 1-5 hours. Similar to the composite studies employed in this study, we compute the maximum of gravity wave activity and perform a composite study. Figure 9a shows the gravity wave composite for the echo top and GLM density. We can see the high variability of the convection with a succession of moments of more intense convection, with a peak of lightning followed by a higher cloud top. Figure 9b shows the composite for the parameters describing the cloud variability, Tir, and the frequencies of Tir < 245 K, a proxy for convective cloud cover, and Tir < 284 K, a proxy for total cloud cover. This figure describes a typical variability in this frequency range. Intracloud or intercloud variability controls convection in Amazonia and consequently the formation or reduction of particles. During thunderstorms, the updrafts advect particles upward, followed by downdrafts advecting cloud content to the surface. This implies particle modulation by in-cloud scavenging of BL particles and by the downdraft bringing air rich in oxidants and/or UFP to the BL. This intermittent series of updrafts/downdrafts modify the particles in the BL in a rich spectrum of processes, dominated by UFP enhancement and reduction of N_{AIT} and N_{ACC} that occur hundreds of minutes before and after the maximum convective events, not continuously but in a high variability environment.

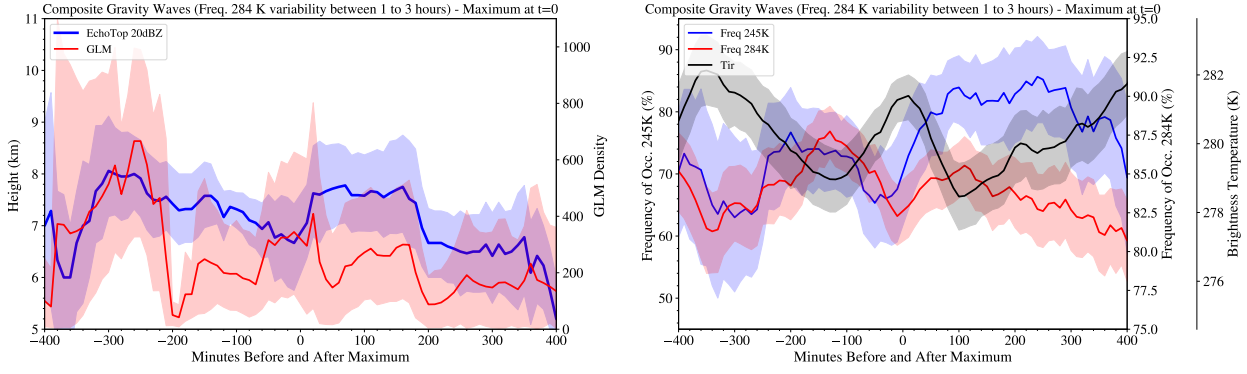

Figure 9. Composite at 400 minutes before and after the maximum of variability in the frequency interval from 1 to 5 hours of the total cloud cover (Tir<284K). a) Echo top and lightning density. b) Tir, frequency of occurrence of Tir< 245 K and Tir<284K in the area of 12 by 12 km^2. The shaded area corresponds to confidence interval of 95%.

3.5 Conceptual Model

The results obtained in this study complement conceptual models of the effects of weather events on particle size distributions in the Amazon. Zhao et al. (2020) discussed the high concentration of ultrafine particles in the upper troposphere (UT)

https://doi.org/10.5194/acp-2021-314
Preprint. Discussion started: 20 April 2021


Atmospheric Chemistry and Physics Discussions

and mentioned that the formation processes are still unknown. They demonstrated that new particle formation in the UT is associated with low volatility organics formed from biogenic emissions from the Amazon forest. Kupc et al. (2020) improved the knowledge about the source of ultrafine particles in the UT, concluding that they are formed in the outflow of mesoscale convective systems. Andreae et al. (2018) described the high concentrations of UFP in the UT based on the ACRIDICON-CHUVA experiment. They suggested that these particles could be transported by downdrafts to form new CCN in the planetary BL by VOC oxidation and growth processes. However, downdrafts from deep convection occur preferentially from below the 10-14 km layer of the source of high concentration of ultrafine particles.

Figure 10 shows the contoured frequency by altitude diagram (CFAD) of the resultant vertical velocity (W) obtained by the RWP at the ATTO-Campina site. The data consist of 54 days of measurements between 16 October and 8 December 2020, the season of the deepest thunderstorms; therefore, it describes the period of maximum extension of the updraft vertical distribution. The vertical resolution of the CFAD is set to 840 m, while the W resolution is $0.1\,\mathrm{m\,s^{-1}}$. Contours are also shown for the number of data points, namely, 250, 750 and 1250 (magenta curves). This figure was built using the RWP and describes the resultant movement between the updraft/downdraft and rain drop terminal velocity. The instrument measures the vertical movement of the rain drops, which is a combination of the droplet terminal velocity and air vertical motion. To provide a reference, Martins et al. (2010) discuss rain droplets in Amazonian region and mention peaks of 0.5, 1.0 and 2.0 mm size distributions for rainfall events, which approximately corresponds to a terminal velocity between 4 and $7\,\mathrm{m\,s^{-1}}$.

However, the main feature to be explored in this figure is not the absolute value of the air vertical velocity, but the layer on which the vertical velocity acts. These data show that downdrafts are mainly located below 10 km, but the layer of maximum concentration of ultrafine particles is mainly above 10 km. Therefore, the ultrafine particles are more prone to be advected through the Hadley and Walker cells to middle latitudes than to return to the surface tropics as discussed in Kida (1983) using a Lagrangian general circulation model of air parcels. However, the concentration of ultrafine particles in the upper troposphere is very high, order of magnitudes higher than the surface ultrafine particles, and therefore, even if the maximum downdraft is below the layer of maximum concentration, the small amount advected downward could be the source of surface ultrafine aerosol particles. Wang et al. (2016) described the phenomenon of sharply increasing N_{UFP} and the simultaneous decrease in the N_{AIT} and N_{ACC} during rainfall events, in agreement with the composite studies presented in this study. They showed high concentrations of UFP in the FT, increasing with height, and proposed that convective downdrafts bring down UFP from the free troposphere into the BL. They suggest that these particles arise from new particle formation in the outflow regions of deep convective systems, followed by condensational and coagulational growth.

https://doi.org/10.5194/acp-2021-314
Preprint. Discussion started: 20 April 2021

Atmospheric Chemistry and Physics Discussions

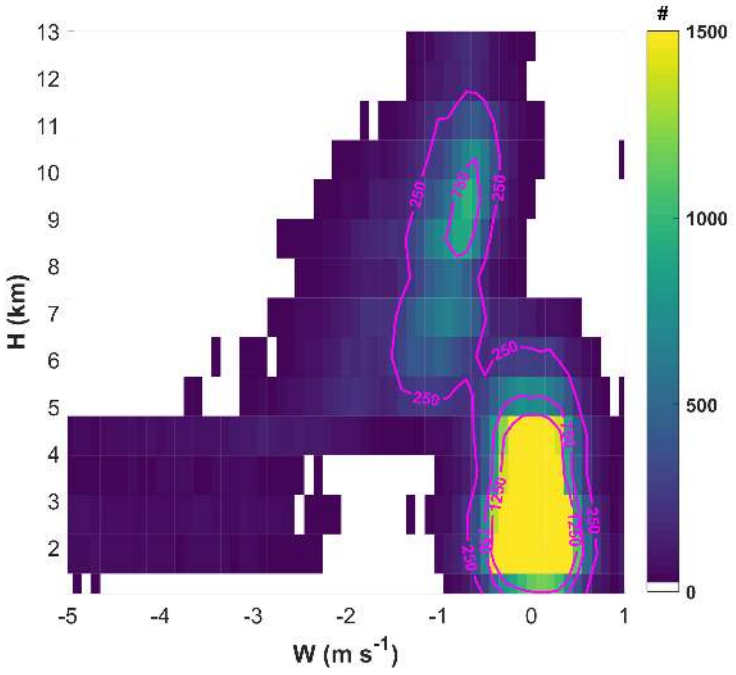

Figure 10. Contoured frequency by altitude diagram of the vertical velocity W obtained by the RWP collected during 54 days of measurements between October 16 and December 8, 2020. The vertical resolution is 840 m, while the W resolution is 0.1 ms^{-1}. The contours show the number of data points, namely, 250, 750 and 1250 (magenta curves).

In any situation, N_{UFP} exhibits a maximum concentration during the night; however, as soon as the sun rises and the convective BL is built, conversion processes to Aitken and accumulation begin, and particle growth occurs up to the time that convection is initiated. Franco et al. (2021) studied ultrafine particle growth and found the most frequent starting cases at approximately twilight time, before the convective BL is developed. Consequently, it is likely that there is a combination of effects, such as the photochemical effect that begins the processes of UFP growing into the Aitken particle size range and the development of the convective BL that contributes to the dynamics of the aerosol (upward advection). In the late afternoon, larger particles start to decrease by rain out, scavenging, and removal by updrafts. This process of increasing UFP and decreasing Aitken and accumulation particles occurs over a large range of variability with successive rain cells, updrafts and downdrafts, controlled by the gravity waves. The rainfall scavenges the larger particles and the associated downdraft contributes to the increase in N_{UFP}.

Related to the seasonal variation, one can note that in the wet season the weather-PSD interaction is stronger than in the dry season. For instance, for the diurnal cycle, the percentage of relative variability of N_{UFP} is similar, but the consequent effect on N_{ACC} is only observed during the wet season. It could be associated with the reduction of concentration during the night followed by a growth process from UFP to ACCP, in the early morning, that is around 30 % in the wet season and nearly imperceptible in the dry season due to the very high absolute concentration of ACCP in the dry season. Also, related to the

https://doi.org/10.5194/acp-2021-314
Preprint. Discussion started: 20 April 2021


Atmospheric Chemistry and Physics Discussions

effect of lightning on PSD, the effect during the dry season is small and shows a small difference among the different types of rainfall events (storm, thunderstorm, the cloud top height,the total liquid water). The dry season is the maximum lighting activity season, but it is in the wet season that a feedback between lighting and N_{ACC} (150 m before the maximum lightning event) is observed. Hernández Pardo et al. (2021) using observation and modeling for Amazonian clouds, concluded that the width of the cloud droplet size distribution for clean clouds (aerosol concentration $< 900\,\mathrm{cm}^{-3}$), varies as function of the adiabaticity of the cloud. However, for polluted clouds (aerosol concentration $> 2000\,\mathrm{cm}^{-3}$), the distribution width is not a function of the adiabaticity, and varies very little. There are clear difference among the seasons as showed in the present study, the high concentration of particles, during the dry season, is relatively less sensitivity to weather conditions than during the wet season, with lower aerosol concentration,where the different types of weather events dominate the weather-PSD interactions.

4 Conclusions

Particle size distribution data from two SMPS instruments at ATTO at 60 and 325 m was combined with satellite and radar data to provide the basis for exploring the relationship between weather events and changes in particle size distributions in the BL of the Central Amazon forest. A colocated time series for ATTO with 10 minutes of resolution was produced, combining the different types of measurements. Several features describing the evolution of the particle size distribution could be observed for different weather cycles, forcings and characteristics.

The seasonality is pronounced, with particle concentrations in the dry season being an order of magnitude larger than that during the wet season, and the brightness temperature followed this behavior, with colder brightness temperatures during the wet season (cold cloud tops) than during the dry season. However, lightning has a completely different behavior, and the transition season is the period where the maximum lightning activity is observed.

The diurnal cycle shows a typical behavior with nearly the same phase in both seasons. The maximum concentration of UFP is observed at sunrise, and at this time, N_{AIT} and N_{ACC} present a minimum. As the sun rises and the convective BL develops, the UFP begin to show a decrease in the number concentration followed by an increase in N_{AIT} and N_{ACC}, with a typical behavior of growth in the particle size. At the end of the afternoon, an inverse situation occurs, and N_{AIT} and N_{ACC} decrease while N_{UFP} increases due to the more intense rainfall. Despite the higher concentration of accumulation particles, it is N_{UFP} that has the larger relative amplitude, except during the wet season in which the concentration of accumulation particles mode also have a significant relative variation.

The composite with the lightning activity describes the typical characteristics of the evolution of particle size changes due to convective rainfall. At approximately 100 minutes before and 200 minutes after the maximum lightning activity, N_{UFP} increases and Aitken and accumulation particles decrease. Another interesting property is the larger number of lightning events when the aerosol background is higher, which appears to be an indication of convective cloud invigoration.

The same behavior for lightning is observed by the composites of the echo top, rain rate (reflectivity at 3 km), integrated cloud liquid water (VIL), and brightness temperature (Tir). Notably, a different behavior is observed between wet and dry seasons. During the wet season, lightning correlates with a greater change in the particle size distribution in comparison with the dry

https://doi.org/10.5194/acp-2021-314
Preprint. Discussion started: 20 April 2021

Atmospheric Chemistry and Physics Discussions

season for the other weather parameters. This feature should be investigated in future campaigns to explain the reasons for this large sensitivity during the wet season. It seems that for small aerosol concentrations weather-PSD interaction is dominated by the weather events, however, during the dry season this interaction is dominated by the total aerosol concentration.

Gravity waves are very important in the convective activity modulation and produce a high variability, making the particle size distribution evolution much more complex and controlling the succession of rain cells, updrafts, and downdrafts.

Finally, using the radar wind profiler at the Campina site, the vertical distribution of the vertical velocity was computed. The data were collected in the season of the most intense convective activity (October – December) and show that downdrafts are mainly located below 10 km, while the layer of maximum concentration of UFP is mainly above 10 km. However, if even a small amount of UFP from the UT is advected downward it could support the concentration of UFP in surface, because N_{UFP} in the upper troposphere is several orders of magnitude higher than at the surface. This study opens new questions that need to be pursued in detail in new field campaigns, such as CAFE-Brazil scheduled for 2022 and the new ATTO-Campina site that provides measurements of atmospheric and cloud physical properties.

Data availability. ATTO data can be found in the ATTO data portal under https://www.attodata.org/ (ATTO, 2020). For data requests beyond the available data, please refer to the corresponding authors.

Appendix A

A1

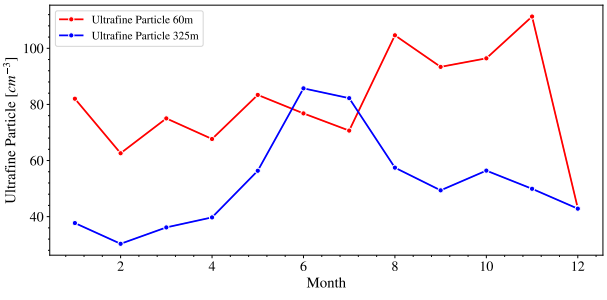

Figure A1. Monthly average N_{UFP} particles at 60 m and 325 m

https://doi.org/10.5194/acp-2021-314
Preprint. Discussion started: 20 April 2021

Atmospheric Chemistry and Physics Discussions

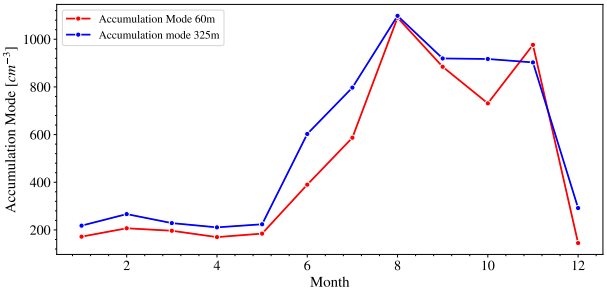

Figure A2. Monthly average accumulation particles at 60 m and 325 m

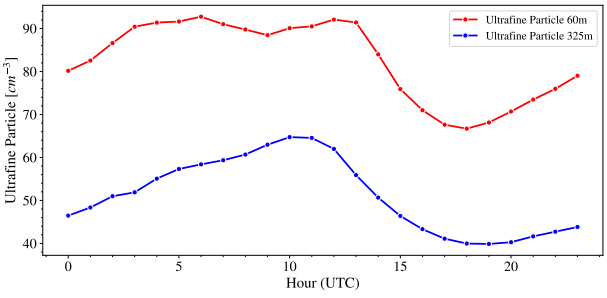

Figure A3. Hourly average N_{UFP} particles at 60 m and 325 m

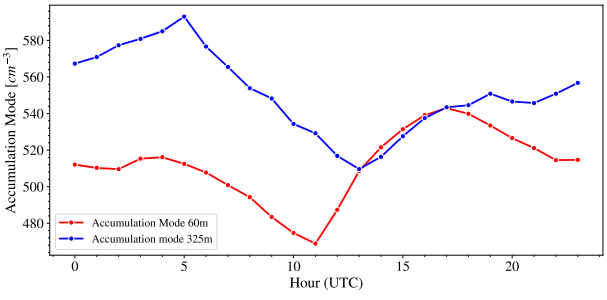

Figure A4. Hourly average accumulation particles at 60 m and 325 m

Author contributions. LATM conceptualized this study, conducted the data analysis and wrote the paper. LAK, MAMF, FD, and BAH conducted the SMPS measurements at ATTO and took care for data quality checks and processing. MLP, PA, and SW supported the ATTO measurements and data analysis. MAC contributed with the LAP3000 data treatment and analysis MOA, UP and CP contributed to the interpretation of the data and finalization of the paper in various discussions. All the authors contributed to the interpretation of the results and writing of the paper.

https://doi.org/10.5194/acp-2021-314
Preprint. Discussion started: 20 April 2021

Atmospheric Chemistry and Physics Discussions

Competing interests. The authors declare that they have no conflict of interest.

Acknowledgements. This research has been supported by the Max Planck Society, the FAPESP grant 2017/17047-0, the Bundesministerium für Bildung und Forschung (BMBF contracts 01LB1001A and 01LK1602B), and the Max Planck Graduate Center with the Johannes Gutenberg University Mainz (MPGC). For the operation of the ATTO site, we acknowledge the support by the Max Planck Society, the German Federal Ministry of Education and Research and the Brazilian Ministério da Ciência, Tecnologia e Inovação as well as the Amazon State University (UEA), FAPEAM, LBA/INPA, and SDS/CEUC/RDS-Uatumã. MAC was supported by FAPESP grant 2020/13273-9. We would like to especially thank all the people involved in the technical, logistical, and scientific support of the ATTO project, in particular Susan Trumbore, Carlos Alberto Quesada, Reiner Ditz, Jürgen Kesselmeier, Thomas Klimach, Björn Nillius, Antonio O. Manzi, Thomas Disper, Hermes Braga Xavier, Nagib Alberto de Castro Souza, Adir Vasconcelos Brandão, Amauri Rodriguês Perreira, André Luiz Matos, Fábio Jorge, Fernando Goncalves Morais, Roberta Pereira de Souza, Bruno Takeshi, Uwe Schultz, Karl Kübler, Olaf Kolle, Martin Hertel, Kerstin Hippler, and Steffen Schmidt. In particular, we would like to thank Delano Campos, Andrew Crozier, Sam Jones, Juarez Viegas, Wallace Rabelo Costa, and Antonio Huxley Melo Nascimento for the frequent maintenance and troubleshooting of the ATTO instruments.

https://doi.org/10.5194/acp-2021-314
Preprint. Discussion started: 20 April 2021

Atmospheric Chemistry and Physics Discussions

References

Adler, R. F. and Mack, R. A.: Thunderstorm cloud top dynamics as inferred from satellite observations and a cloud top parcel model., 1986.

Albrecht, B. A.: Aerosols, Cloud Microphysics, and Fractional Cloudiness, Science, 245, 1227–1230, https://doi.org/10.1126/science.245.4923.1227, https://science.sciencemag.org/content/245/4923/1227, 1989.

Alexander, M. J., Holton, J. R., and Durran, D. R.: The Gravity Wave Response above Deep Convection in a Squall Line Simulation, Journal of Atmospheric Sciences, 52, 2212 – 2226, https://doi.org/10.1175/1520-0469(1995)052<2212:TGWRAD>2.0.CO;2, https://journals.ametsoc.org/view/journals/atsc/52/12/1520-0469_1995_052_2212_tgwrad_2_0_co_2.xml, 1995.

Andreae, M. O.: Correlation between cloud condensation nuclei concentration and aerosol optical thickness in remote and polluted regions, Atmospheric Chemistry and Physics, 9, 543–556, <GotoISI>://WOS:000263325700013, 2009.

Andreae, M. O., Rosenfeld, D., Artaxo, P., Costa, A. A., Frank, G. P., Longo, K. M., and Silva-Dias, M. A. F.: Smoking Rain Clouds over the Amazon, Science, 303, 1337–1342, https://doi.org/10.1126/science.1092779, https://science.sciencemag.org/content/303/5662/1337, 2004.

Andreae, M. O., Acevedo, O. C., Araùjo, A., Artaxo, P., Barbosa, C. G. G., Barbosa, H. M. J., Brito, J., Carbone, S., Chi, X., Cintra, B. B. L., da Silva, N. F., Dias, N. L., Dias-Júnior, C. Q., Ditas, F., Ditz, R., Godoi, A. F. L., Godoi, R. H. M., Heimann, M., Hoffmann, T., Kesselmeier, J., Könemann, T., Krüger, M. L., Lavric, J. V., Manzi, A. O., Lopes, A. P., Martins, D. L., Mikhailov, E. F., Moran-Zuloaga, D., Nelson, B. W., Nölscher, A. C., Santos Nogueira, D., Piedade, M. T. F., Pöhlker, C., Pöschl, U., Quesada, C. A., Rizzo, L. V., Ro, C.-U., Ruckteschler, N., Sá, L. D. A., de Oliveira Sá, M., Sales, C. B., dos Santos, R. M. N., Saturno, J., Schöngart, J., Sörgel, M., de Souza, C. M., de Souza, R. A. F., Su, H., Targhetta, N., Tóta, J., Trebs, I., Trumbore, S., van Eijck, A., Walter, D., Wang, Z., Weber, B., Williams, J., Winderlich, J., Wittmann, F., Wolff, S., and Yáñez Serrano, A. M.: The Amazon Tall Tower Observatory (ATTO): overview of pilot measurements on ecosystem ecology, meteorology, trace gases, and aerosols, Atmospheric Chemistry and Physics, 15, 10 723–10 776, https://doi.org/10.5194/acp-15-10723-2015, https://acp.copernicus.org/articles/15/10723/2015/, 2015.

Andreae, M. O., Afchine, A., Albrecht, R., Holanda, B. A., Artaxo, P., Barbosa, H. M. J., Borrmann, S., Cecchini, M. A., Costa, A., Dollner, M., Fütterer, D., Järvinen, E., Jurkat, T., Klimach, T., Konemann, T., Knote, C., Krämer, M., Krisna, T., Machado, L. A. T., Mertes, S., Minikin, A., Pöhlker, C., Pöhlker, M. L., Pöschl, U., Rosenfeld, D., Sauer, D., Schlager, H., Schnaiter, M., Schneider, J., Schulz, C., Spanu, A., Sperling, V. B., Voigt, C., Walser, A., Wang, J., Weinzierl, B., Wendisch, M., and Ziereis, H.: Aerosol characteristics and particle production in the upper troposphere over the Amazon Basin, Atmospheric Chemistry and Physics, 18, 921–961, https://doi.org/10.5194/acp-18-921-2018, https://acp.copernicus.org/articles/18/921/2018/, 2018.

Angevine, W. M., Edwards, J. M., Lothon, M., LeMone, M. A., and Osborne, S. R.: Transition Periods in the Diurnally-Varying Atmospheric Boundary Layer Over Land, Boundary-Layer Meteorology, pp. 1–19, 2020.

Artaxo, P., Hansson, H.-C., Andreae, M. O., Bäck, J., Alves, E. G., Barbosa, H. M. J., , et al.: Tropical and Boreal Forest – Atmosphere Interactions: a Review, submitted to Tellus, 2021.

Betts, A. K., Fuentes, J. D., Garstang, M., and Ball, J. H.: Surface diurnal cycle and boundary layer structure over Rondônia during the rainy season, Journal of Geophysical Research: Atmospheres, 107, LBA 32–1–LBA 32–14, https://doi.org/https://doi.org/10.1029/2001JD000356, https://agupubs.onlinelibrary.wiley.com/doi/abs/10.1029/2001JD000356, 2002.

Boschat, G., Simmonds, I., Purich, A., Cowan, T., and Pezza, A. B.: On the use of composite analyses to form physical hypotheses: An example from heat wave – SST associations, Scientific Reports, 6, 29 599, https://doi.org/10.1038/srep29599, https://doi.org/10.1038/srep29599, 2016.

https://doi.org/10.5194/acp-2021-314
Preprint. Discussion started: 20 April 2021

Atmospheric Chemistry and Physics Discussions

Carneiro, R. G. and Fisch, G.: Observational analysis of the daily cycle of the planetary boundary layer in the central Amazon during a non-El Niño year and El Niño year (GoAmazon project 2014/5), Atmospheric Chemistry and Physics, 20, 5547–5558, https://doi.org/10.5194/acp-20-5547-2020, https://acp.copernicus.org/articles/20/5547/2020/, 2020.

Cecchini, M. A., Machado, L. A. T., Andreae, M. O., Martin, S. T., Albrecht, R. I., Artaxo, P., Barbosa, H. M. J., Borrmann, S., Fütterer, D., Jurkat, T., Mahnke, C., Minikin, A., Molleker, S., Pöhlker, M. L., Pöschl, U., Rosenfeld, D., Voigt, C., Weinzierl, B., and Wendisch, M.: Sensitivities of Amazonian clouds to aerosols and updraft speed, Atmospheric Chemistry and Physics, 17, 10 037–10 050, https://doi.org/10.5194/acp-17-10037-2017, https://acp.copernicus.org/articles/17/10037/2017/, 2017a.

Cecchini, M. A., Machado, L. A. T., Wendisch, M., Costa, A., Krämer, M., Andreae, M. O., Afchine, A., Albrecht, R. I., Artaxo, P., Borrmann, S., Fütterer, D., Klimach, T., Mahnke, C., Martin, S. T., Minikin, A., Molleker, S., Pardo, L. H., Pöhlker, C., Pöhlker, M. L., Pöschl, U., Rosenfeld, D., and Weinzierl, B.: Illustration of microphysical processes in Amazonian deep convective clouds in the gamma phase space: introduction and potential applications, Atmospheric Chemistry and Physics, 17, 14 727–14 746, https://doi.org/10.5194/acp-17-14727-2017, https://acp.copernicus.org/articles/17/14727/2017/, 2017b.

Deierling, W. and Petersen, W. A.: Total lightning activity as an indicator of updraft characteristics, Journal of Geophysical Research: Atmospheres, 113, https://doi.org/https://doi.org/10.1029/2007JD009598, https://agupubs.onlinelibrary.wiley.com/doi/abs/10.1029/2007JD009598, 2008.

Fan, J., Rosenfeld, D., Zhang, Y., Giangrande, S. E., Li, Z., Machado, L. A. T., Martin, S. T., Yang, Y., Wang, J., Artaxo, P., Barbosa, H. M. J., Braga, R. C., Comstock, J. M., Feng, Z., Gao, W., Gomes, H. B., Mei, F., Pöhlker, C., Pöhlker, M. L., Pöschl, U., and de Souza, R. A. F.: Substantial convection and precipitation enhancements by ultrafine aerosol particles, Science, 359, 411–418, https://doi.org/10.1126/science.aan8461, https://science.sciencemag.org/content/359/6374/411, 2018.

Fisch, G., Tota, J., Machado, L. A. T., Silva Dias, M. A. F., da F. Lyra, R. F., Nobre, C. A., Dolman, A. J., and Gash, J. H. C.: The convective boundary layer over pasture and forest in Amazonia, Theoretical and Applied Climatology, 78, 47–59, https://doi.org/10.1007/s00704-004-0043-x, https://doi.org/10.1007/s00704-004-0043-x, 2004.

Franco, M. A., Ditas, F., Machado, L. A. T., Kremper, L. A., Rizzo, L. V., , et al.: Occurrence of ultrafine particle growth events in the Amazon rain forest, being submit to Atmospheric Chemistry and Physics, 2021.

Gerken, T., Wei, D., Chase, R. J., Fuentes, J. D., Schumacher, C., Machado, L. A., Andreoli, R. V., Chamecki, M., Ferreira de Souza, R. A., Freire, L. S., Jardine, A. B., Manzi, A. O., Nascimento dos Santos, R. M., von Randow, C., dos Santos Costa, P., Stoy, P. C., Tóta, J., and Trowbridge, A. M.: Downward transport of ozone rich air and implications for atmospheric chemistry in the Amazon rainforest, Atmospheric Environment, 124, 64 – 76, https://doi.org/https://doi.org/10.1016/j.atmosenv.2015.11.014, http://www.sciencedirect.com/science/article/pii/S1352231015305227, 2016.

Giangrande, S. E., Feng, Z., Jensen, M. P., Comstock, J. M., Johnson, K. L., Toto, T., Wang, M., Burleyson, C., Bharadwaj, N., Mei, F., Machado, L. A. T., Manzi, A. O., Xie, S., Tang, S., Silva Dias, M. A. F., de Souza, R. A. F., Schumacher, C., and Martin, S. T.: Cloud characteristics, thermodynamic controls and radiative impacts during the Observations and Modeling of the Green Ocean Amazon (GoAmazon2014/5) experiment, Atmospheric Chemistry and Physics, 17, 14 519–14 541, https://doi.org/10.5194/acp-17-14519-2017, https://acp.copernicus.org/articles/17/14519/2017/, 2017.

Goodman, S. J., Blakeslee, R. J., Koshak, W. J., Mach, D., Bailey, J., Buechler, D., Carey, L., Schultz, C., Bateman, M., McCaul, E., and Stano, G.: The GOES-R Geostationary Lightning Mapper (GLM), Atmospheric Research, 125-126, 34 – 49, https://doi.org/https://doi.org/10.1016/j.atmosres.2013.01.006, http://www.sciencedirect.com/science/article/pii/S0169809513000434, 2013.

https://doi.org/10.5194/acp-2021-314
Preprint. Discussion started: 20 April 2021

Greene, D. R. and Clark, R. A.: Vertically Integrated Liquid Water—A New Analysis Tool, Monthly Weather Review, 100, 548 – 552, https://doi.org/10.1175/1520-0493(1972)100<0548:VILWNA>2.3.CO;2, https://journals.ametsoc.org/view/journals/mwre/100/7/1520-0493_1972_100_0548_vilwna_2_3_co_2.xml, 1972.

Grimsdell, A. W., Alexander, M. J., May, P. T., and Hoffmann, L.: Model Study of Waves Generated by Convection with Direct Validation via Satellite, Journal of the Atmospheric Sciences, 67, 1617 – 1631, https://doi.org/10.1175/2009JAS3197.1, https://journals.ametsoc.org/view/journals/atsc/67/5/2009jas3197.1.xml, 2010.

Hansen, J., Sato, M., and Ruedy, R.: Radiative forcing and climate response, Journal of Geophysical Research: Atmospheres, 102, 6831–6864, https://doi.org/https://doi.org/10.1029/96JD03436, https://agupubs.onlinelibrary.wiley.com/doi/abs/10.1029/96JD03436, 1997.

Haywood, J. and Boucher, O.: Estimates of the direct and indirect radiative forcing due to tropospheric aerosols: A review, Reviews of Geophysics, 38, 513–543, https://doi.org/https://doi.org/10.1029/1999RG000078, https://agupubs.onlinelibrary.wiley.com/doi/abs/10.1029/1999RG000078, 2000.

Heikenfeld, M., White, B., Labbouz, L., and Stier, P.: Aerosol effects on deep convection: the propagation of aerosol perturbations through convective cloud microphysics, Atmospheric Chemistry and Physics, 19, 2601–2627, https://doi.org/10.5194/acp-19-2601-2019, https://acp.copernicus.org/articles/19/2601/2019/, 2019.

Henkes, A., Fisch, G., Toledo Machado, L. A., and Chaboureau, J.-P.: Morning boundary layer conditions for shallow to deep convective cloud evolution during the dry season in the central Amazon, Atmospheric Chemistry and Physics Discussions, 2021, 1–29, https://doi.org/10.5194/acp-2021-87, https://acp.copernicus.org/preprints/acp-2021-87/, 2021.

Hernández Pardo, L., Machado, L. A. T., Morrison, H., Cecchini, M., Braga, R., Pöhlker, C., Pöschl, U., Rosenfeld, D., Vendrasco, E., and Pöhlker, M.: Study of the variability of droplet spectral dispersion in convective clouds based on observations and numerical simulations, Atmospheric Chemistry and Physics, 2021.

Holanda, B. A., Pöhlker, M. L., Walter, D., Saturno, J., Sörgel, M., Ditas, J., Ditas, F., Schulz, C., Franco, M. A., Wang, Q., Donth, T., Artaxo, P., Barbosa, H. M. J., Borrmann, S., Braga, R., Brito, J., Cheng, Y., Dollner, M., Kaiser, J. W., Klimach, T., Knote, C., Krüger, O. O., Fütterer, D., Lavrič, J. V., Ma, N., Machado, L. A. T., Ming, J., Morais, F. G., Paulsen, H., Sauer, D., Schlager, H., Schneider, J., Su, H., Weinzierl, B., Walser, A., Wendisch, M., Ziereis, H., Zöger, M., Pöschl, U., Andreae, M. O., and Pöhlker, C.: Influx of African biomass burning aerosol during the Amazonian dry season through layered transatlantic transport of black carbon-rich smoke, Atmospheric Chemistry and Physics, 20, 4757–4785, https://doi.org/10.5194/acp-20-4757-2020, https://acp.copernicus.org/articles/20/4757/2020/, 2020.

IPCC: Summary for Policymakers, book section SPM, p. 1–30, Cambridge University Press, Cambridge, United Kingdom and New York, NY, USA, https://doi.org/10.1017/CBO9781107415324.004, www.climatechange2013.org, 2013.

Jadhav, D. B., Londhe, A. L., and Bose, S.: Observations of NO2 and O3 during thunderstorm activity using visible spectroscopy, Advances in Atmospheric Sciences, 13, 359–374, https://doi.org/10.1007/BF02656853, https://doi.org/10.1007/BF02656853, 1996.

Junk, W. J., Piedade, M. T. F., Schöngart, J., Cohn-Haft, M., Adeney, J. M., and Wittmann, F.: A classification of major naturally-occurring Amazonian lowland wetlands, Wetlands, 31, 623–640, 2011.

Kida, H.: General Circulation of Air Parcels and Transport Characteristics Derived from a Hemispheric GCM, Journal of the Meteorological Society of Japan. Ser. II, 61, 510–523, https://doi.org/10.2151/jmsj1965.61.4_510, 1983.

Koren, I., Kaufman, Y. J., Rosenfeld, D., Remer, L. A., and Rudich, Y.: Aerosol invigoration and restructuring of Atlantic convective clouds, Geophysical Research Letters, 32, https://doi.org/https://doi.org/10.1029/2005GL023187, https://agupubs.onlinelibrary.wiley.com/doi/abs/10.1029/2005GL023187, 2005.

https://doi.org/10.5194/acp-2021-314
Preprint. Discussion started: 20 April 2021

Kupc, A., Williamson, C. J., Hodshire, A. L., Kazil, J., Ray, E., Bui, T. P., Dollner, M., Froyd, K. D., McKain, K., Rollins, A., Schill, G. P., Thames, A., Weinzierl, B. B., Pierce, J. R., and Brock, C. A.: The potential role of organics in new particle formation and initial growth in the remote tropical upper troposphere, Atmospheric Chemistry and Physics, 20, 15 037–15 060, https://doi.org/10.5194/acp-20-15037-2020, https://acp.copernicus.org/articles/20/15037/2020/, 2020.

Lane, T. P. and Zhang, F.: Coupling between Gravity Waves and Tropical Convection at Mesoscales, Journal of the Atmospheric Sciences, 68, 2582 – 2598, https://doi.org/10.1175/2011JAS3577.1, https://journals.ametsoc.org/view/journals/atsc/68/11/2011jas3577.1.xml, 2011.

Leppla, D., Zannoni, N., Kremper, L., Williams, J., Pöhlker, C., Sá, M., Solci, M. C., and Hoffmann, T.: Varying chiral ratio of Pinic acid enantiomers above the Amazon rainforest, Atmospheric Chemistry and Physics Discussions, 2021, 1–19, https://doi.org/10.5194/acp-2021-150, https://acp.copernicus.org/preprints/acp-2021-150/, 2021.

Machado, L. A. T. and Rossow, W. B.: Structural Characteristics and Radiative Properties of Tropical Cloud Clusters, Monthly Weather Review, 121, 3234 – 3260, https://doi.org/10.1175/1520-0493(1993)121<3234:SCARPO>2.0.CO;2, https://journals.ametsoc.org/view/journals/mwre/121/12/1520-0493_1993_121_3234_scarpo_2_0_co_2.xml, 1993.

Machado, L. A. T., Laurent, H., and Lima, A. A.: Diurnal march of the convection observed during TRMM-WETAMC/LBA, Journal of Geophysical Research: Atmospheres, 107, LBA 31–1–LBA 31–15, https://doi.org/https://doi.org/10.1029/2001JD000338, https://agupubs.onlinelibrary.wiley.com/doi/abs/10.1029/2001JD000338, 2002.

Machado, L. A. T., Laurent, H., Dessay, N., and Miranda, I.: Seasonal and diurnal variability of convection over the Amazonia: A comparison of different vegetation types and large scale forcing, Theoretical and Applied Climatology, 78, 61–77, https://doi.org/10.1007/s00704-004-0044-9, https://doi.org/10.1007/s00704-004-0044-9, 2004.

Machado, L. A. T., Calheiros, A. J. P., Biscaro, T., Giangrande, S., Silva Dias, M. A. F., Cecchini, M. A., Albrecht, R., Andreae, M. O., Araujo, W. F., Artaxo, P., Borrmann, S., Braga, R., Burleyson, C., Eichholz, C. W., Fan, J., Feng, Z., Fisch, G. F., Jensen, M. P., Martin, S. T., Pöschl, U., Pöhlker, C., Pöhlker, M. L., Ribaud, J.-F., Rosenfeld, D., Saraiva, J. M. B., Schumacher, C., Thalman, R., Walter, D., and Wendisch, M.: Overview: Precipitation characteristics and sensitivities to environmental conditions during GoAmazon2014/5 and ACRIDICON-CHUVA, Atmospheric Chemistry and Physics, 18, 6461–6482, https://doi.org/10.5194/acp-18-6461-2018, https://acp.copernicus.org/articles/18/6461/2018/, 2018.

Martin, S. T., Artaxo, P., Machado, L. A. T., Manzi, A. O., Souza, R. A. F., Schumacher, C., Wang, J., Andreae, M. O., Barbosa, H. M. J., Fan, J., Fisch, G., Goldstein, A. H., Guenther, A., Jimenez, J. L., Pöschl, U., Silva Dias, M. A., Smith, J. N., and Wendisch, M.: Introduction: Observations and Modeling of the Green Ocean Amazon (GoAmazon2014/5), Atmospheric Chemistry and Physics, 16, 4785–4797, https://doi.org/10.5194/acp-16-4785-2016, https://acp.copernicus.org/articles/16/4785/2016/, 2016.

Martin, S. T., Artaxo, P., Machado, L., Manzi, A. O., Souza, R. A. F., Schumacher, C., Wang, J., Biscaro, T., Brito, J., Calheiros, A., Jardine, K., Medeiros, A., Portela, B., de Sá, S. S., Adachi, K., Aiken, A. C., Albrecht, R., Alexander, L., Andreae, M. O., Barbosa, H. M. J., Buseck, P., Chand, D., Comstock, J. M., Day, D. A., Dubey, M., Fan, J., Fast, J., Fisch, G., Fortner, E., Giangrande, S., Gilles, M., Goldstein, A. H., Guenther, A., Hubbe, J., Jensen, M., Jimenez, J. L., Keutsch, F. N., Kim, S., Kuang, C., Laskin, A., McKinney, K., Mei, F., Miller, M., Nascimento, R., Pauliquevis, T., Pekour, M., Peres, J., Petäjä, T., Pöhlker, C., Pöschl, U., Rizzo, L., Schmid, B., Shilling, J. E., Dias, M. A. S., Smith, J. N., Tomlinson, J. M., Tóta, J., and Wendisch, M.: The Green Ocean Amazon Experiment (GoAmazon2014/5) Observes Pollution Affecting Gases, Aerosols, Clouds, and Rainfall over the Rain Forest, Bulletin of the American Meteorological Society, 98, 981–997, https://doi.org/10.1175/BAMS-D-15-00221.1, https://doi.org/10.1175/BAMS-D-15-00221.1, 2017.

https://doi.org/10.5194/acp-2021-314
Preprint. Discussion started: 20 April 2021

Atmospheric Chemistry and Physics Discussions

Martins, R. C., Machado, L. A., and Costa, A. A.: Characterization of the microphysics of precipitation over Amazon region using radar and disdrometer data, Atmospheric Research, 96, 388 – 394, https://doi.org/https://doi.org/10.1016/j.atmosres.2010.01.011, http://www.sciencedirect.com/science/article/pii/S0169809510000220, 15th International Conference on Clouds and Precipitation, 2010.

Miller, S. D., Straka, W. C., Yue, J., Smith, S. M., Alexander, M. J., Hoffmann, L., Setvák, M., and Partain, P. T.: Upper atmospheric gravity wave details revealed in nightglow satellite imagery, Proceedings of the National Academy of Sciences, 112, E6728–E6735, https://doi.org/10.1073/pnas.1508084112, https://www.pnas.org/content/112/49/E6728, 2015.

Moran-Zuloaga, D., Ditas, F., Walter, D., Saturno, J., Brito, J., Carbone, S., Chi, X., Hrabě de Angelis, I., Baars, H., Godoi, R. H. M., Heese, B., Holanda, B. A., Lavrič, J. V., Martin, S. T., Ming, J., Pöhlker, M. L., Ruckteschler, N., Su, H., Wang, Y., Wang, Q., Wang, Z., Weber, B., Wolff, S., Artaxo, P., Pöschl, U., Andreae, M. O., and Pöhlker, C.: Long-term study on coarse mode aerosols in the Amazon rain forest with the frequent intrusion of Saharan dust plumes, Atmospheric Chemistry and Physics, 18, 10 055–10 088, https://doi.org/10.5194/acp-18-10055-2018, https://acp.copernicus.org/articles/18/10055/2018/, 2018.

Palm, B. B., de Sá, S. S., Day, D. A., Campuzano-Jost, P., Hu, W., Seco, R., Sjostedt, S. J., Park, J.-H., Guenther, A. B., Kim, S., Brito, J., Wurm, F., Artaxo, P., Thalman, R., Wang, J., Yee, L. D., Wernis, R., Isaacman-VanWertz, G., Goldstein, A. H., Liu, Y., Springston, S. R., Souza, R., Newburn, M. K., Alexander, M. L., Martin, S. T., and Jimenez, J. L.: Secondary organic aerosol formation from ambient air in an oxidation flow reactor in central Amazonia, Atmospheric Chemistry and Physics, 18, 467–493, https://doi.org/10.5194/acp-18-467-2018, https://acp.copernicus.org/articles/18/467/2018/, 2018.

Pöhlker, M. L., Pöhlker, C., Ditas, F., Klimach, T., Hrabe de Angelis, I., Araújo, A., Brito, J., Carbone, S., Cheng, Y., Chi, X., Ditz, R., Gunthe, S. S., Kesselmeier, J., Könemann, T., Lavrič, J. V., Martin, S. T., Mikhailov, E., Moran-Zuloaga, D., Rose, D., Saturno, J., Su, H., Thalman, R., Walter, D., Wang, J., Wolff, S., Barbosa, H. M. J., Artaxo, P., Andreae, M. O., and Pöschl, U.: Long-term observations of cloud condensation nuclei in the Amazon rain forest – Part 1: Aerosol size distribution, hygroscopicity, and new model parametrizations for CCN prediction, Atmospheric Chemistry and Physics, 16, 15 709–15 740, https://doi.org/10.5194/acp-16-15709-2016, https://acp.copernicus.org/articles/16/15709/2016/, 2016.

Pöhlker, M. L., Ditas, F., Saturno, J., Klimach, T., Hrabě de Angelis, I., Araùjo, A. C., Brito, J., Carbone, S., Cheng, Y., Chi, X., Ditz, R., Gunthe, S. S., Holanda, B. A., Kandler, K., Kesselmeier, J., Könemann, T., Krüger, O. O., Lavrič, J. V., Martin, S. T., Mikhailov, E., Moran-Zuloaga, D., Rizzo, L. V., Rose, D., Su, H., Thalman, R., Walter, D., Wang, J., Wolff, S., Barbosa, H. M. J., Artaxo, P., Andreae, M. O., Pöschl, U., and Pöhlker, C.: Long-term observations of cloud condensation nuclei over the Amazon rain forest – Part 2: Variability and characteristics of biomass burning, long-range transport, and pristine rain forest aerosols, Atmospheric Chemistry and Physics, 18, 10 289–10 331, https://doi.org/10.5194/acp-18-10289-2018, https://acp.copernicus.org/articles/18/10289/2018/, 2018.

Pöschl, U., Martin, S. T., Sinha, B., Chen, Q., Gunthe, S. S., Huffman, J. A., Borrmann, S., Farmer, D. K., Garland, R. M., Helas, G., Jimenez, J. L., King, S. M., Manzi, A., Mikhailov, E., Pauliquevis, T., Petters, M. D., Prenni, A. J., Roldin, P., Rose, D., Schneider, J., Su, H., Zorn, S. R., Artaxo, P., and Andreae, M. O.: Rainforest Aerosols as Biogenic Nuclei of Clouds and Precipitation in the Amazon, Science, 329, 1513–1516, https://doi.org/10.1126/science.1191056, https://science.sciencemag.org/content/329/5998/1513, 2010.

Ramanathan, V., Crutzen, P. J., Kiehl, J. T., and Rosenfeld, D.: Aerosols, Climate, and the Hydrological Cycle, Science, 294, 2119–2124, https://doi.org/10.1126/science.1064034, https://science.sciencemag.org/content/294/5549/2119, 2001.

https://doi.org/10.5194/acp-2021-314
Preprint. Discussion started: 20 April 2021

Rosenfeld, D.: TRMM observed first direct evidence of smoke from forest fires inhibiting rainfall, Geophysical Research Letters, 26, 3105–3108, https://doi.org/https://doi.org/10.1029/1999GL006066, https://agupubs.onlinelibrary.wiley.com/doi/abs/10.1029/1999GL006066, 1999.

Rosenfeld, D.: Chapter 6 – Cloud-Aerosol-Precipitation Interactions Based of Satellite Retrieved Vertical Profiles of Cloud Microstructure, in: Remote Sensing of Aerosols, Clouds, and Precipitation, 2018.

Rosenfeld, D., Lohmann, U., Raga, G. B., O'Dowd, C. D., Kulmala, M., Fuzzi, S., Reissell, A., and Andreae, M. O.: Flood or Drought: How Do Aerosols Affect Precipitation?, Science, 321, 1309–1313, https://doi.org/10.1126/science.1160606, https://science.sciencemag.org/content/321/5894/1309, 2008.

Saturno, J., Holanda, B. A., Pöhlker, C., Ditas, F., Wang, Q., Moran-Zuloaga, D., Brito, J., Carbone, S., Cheng, Y., Chi, X., Ditas, J., Hoffmann, T., Hrabe de Angelis, I., Könemann, T., Lavrič, J. V., Ma, N., Ming, J., Paulsen, H., Pöhlker, M. L., Rizzo, L. V., Schlag, P., Su, H., Walter, D., Wolff, S., Zhang, Y., Artaxo, P., Pöschl, U., and Andreae, M. O.: Black and brown carbon over central Amazonia: long-term aerosol measurements at the ATTO site, Atmospheric Chemistry and Physics, 18, 12 817–12 843, https://doi.org/10.5194/acp-18-12817-2018, https://acp.copernicus.org/articles/18/12817/2018/, 2018.

Schrod, J., Thomson, E. S., Weber, D., Kossmann, J., Pöhlker, C., Saturno, J., Ditas, F., Artaxo, P., Clouard, V., Saurel, J.-M., Ebert, M., Curtius, J., and Bingemer, H. G.: Long-term deposition and condensation ice-nucleating particle measurements from four stations across the globe, Atmospheric Chemistry and Physics, 20, 15 983–16 006, https://doi.org/10.5194/acp-20-15983-2020, https://acp.copernicus.org/articles/20/15983/2020/, 2020.

Schulz, C., Schneider, J., Amorim Holanda, B., Appel, O., Costa, A., de Sá, S. S., Dreiling, V., Fütterer, D., Jurkat-Witschas, T., Klimach, T., Knote, C., Krämer, M., Martin, S. T., Mertes, S., Pöhlker, M. L., Sauer, D., Voigt, C., Walser, A., Weinzierl, B., Ziereis, H., Zöger, M., Andreae, M. O., Artaxo, P., Machado, L. A. T., Pöschl, U., Wendisch, M., and Borrmann, S.: Aircraft-based observations of isoprene-epoxydiol-derived secondary organic aerosol (IEPOX-SOA) in the tropical upper troposphere over the Amazon region, Atmospheric Chemistry and Physics, 18, 14 979–15 001, https://doi.org/10.5194/acp-18-14979-2018, https://acp.copernicus.org/articles/18/14979/2018/, 2018.

Stull, R. B.: An Introduction to Boundary Layer Meteorology, Springer, Dordrecht, https://doi.org/10.1007/978-94-009-3027-8, 1988.

Tridon, F., Battaglia, A., Kollias, P., Luke, E., and Williams, C. R.: Signal Postprocessing and Reflectivity Calibration of the Atmospheric Radiation Measurement Program 915-MHz Wind Profilers, Journal of Atmospheric and Oceanic Technology, 30, 1038 – 1054, https://doi.org/10.1175/JTECH-D-12-00146.1, https://journals.ametsoc.org/view/journals/atot/30/6/jtech-d-12-00146_1.xml, 2013.

Tuch, T. M., Haudek, A., Müller, T., Nowak, A., Wex, H., and Wiedensohler, A.: Design and performance of an automatic regenerating adsorption aerosol dryer for continuous operation at monitoring sites, Atmospheric Measurement Techniques, 2, 417–422, https://doi.org/10.5194/amt-2-417-2009, https://amt.copernicus.org/articles/2/417/2009/, 2009.

Twomey, S. and Warner, J.: Comparison of Measurements of Cloud Droplets and Cloud Nuclei, Journal of Atmospheric Sciences, 24, 702 – 703, https://doi.org/10.1175/1520-0469(1967)024<0702:COMOCD>2.0.CO;2, https://journals.ametsoc.org/view/journals/atsc/24/6/1520-0469_1967_024_0702_comocd_2_0_co_2.xml, 1967.

Varanda Rizzo, L., Roldin, P., Brito, J., Backman, J., Swietlicki, E., Krejci, R., Tunved, P., Petäjä, T., Kulmala, M., and Artaxo, P.: Multi-year statistical and modeling analysis of submicrometer aerosol number size distributions at a rain forest site in Amazonia, Atmospheric Chemistry and Physics, 18, 10 255–10 274, https://doi.org/10.5194/acp-18-10255-2018, https://acp.copernicus.org/articles/18/10255/2018/, 2018.

https://doi.org/10.5194/acp-2021-314
Preprint. Discussion started: 20 April 2021


Atmospheric Chemistry and Physics Discussions

von der Weiden, S.-L., Drewnick, F., and Borrmann, S.: Particle Loss Calculator – a new software tool for the assessment of the performance of aerosol inlet systems, Atmospheric Measurement Techniques, 2, 479–494, https://doi.org/10.5194/amt-2-479-2009, https://amt.copernicus.org/articles/2/479/2009/, 2009.

Wang, J., Krejci, R., Giangrande, S., Kuang, C., Barbosa, H. M., Brito, J., Carbone, S., Chi, X., Comstock, J., Ditas, F., et al.: Amazon boundary layer aerosol concentration sustained by vertical transport during rainfall, Nature, 539, 416–419, https://doi.org/10.1038/nature19819, https://doi.org/10.1038/nature19819, 2016.

Wang, P. K.: The thermodynamic structure atop a penetrating convective thunderstorm, Atmospheric Research, 83, 254 – 262, https://doi.org/https://doi.org/10.1016/j.atmosres.2005.08.010, http://www.sciencedirect.com/science/article/pii/S0169809506001116, european Conference on Severe Storms 2004, 2007.

Wendisch, M., P?schl, U., Andreae, M. O., Machado, L. A. T., Albrecht, R., Schlager, H., Rosenfeld, D., Martin, S. T., Abdelmonem, A., Afchine, A., Ara?jo, A. C., Artaxo, P., Aufmhoff, H., Barbosa, H. M. J., Borrmann, S., Braga, R., Buchholz, B., Cecchini, M. A., Costa, A., Curtius, J., Dollner, M., Dorf, M., Dreiling, V., Ebert, V., Ehrlich, A., Ewald, F., Fisch, G., Fix, A., Frank, F., F?tterer, D., Heckl, C., Heidelberg, F., H?neke, T., J?kel, E., J?rvinen, E., Jurkat, T., Kanter, S., K?stner, U., Kenntner, M., Kesselmeier, J., Klimach, T., Knecht, M., Kohl, R., K?lling, T., Kr?mer, M., Kr?ger, M., Krisna, T. C., Lavric, J. V., Longo, K., Mahnke, C., Manzi, A. O., Mayer, B., Mertes, S., Minikin, A., Molleker, S., M?nch, S., Nillius, B., Pfeilsticker, K., P?hlker, C., Roiger, A., Rose, D., Rosenow, D., Sauer, D., Schnaiter, M., Schneider, J., Schulz, C., de Souza, R. A. F., Spanu, A., Stock, P., Vila, D., Voigt, C., Walser, A., Walter, D., Weigel, R., Weinzierl, B., Werner, F., Yamasoe, M. A., Ziereis, H., Zinner, T., and Z?ger, M.: ACRIDICON?CHUVA Campaign: Studying Tropical Deep Convective Clouds and Precipitation over Amazonia Using the New German Research Aircraft HALO, Bulletin of the American Meteorological Society, 97, 1885 – 1908, https://doi.org/10.1175/BAMS-D-14-00255.1, https://journals.ametsoc.org/view/journals/bams/97/10/bams-d-14-00255.1.xml, 2016.

Williamson, C. J., Kupc, A., Axisa, D., Bilsback, K. R., Bui, T., Campuzano-Jost, P., Dollner, M., Froyd, K. D., Hodshire, A. L., Jimenez, J. L., Kodros, J. K., Luo, G., Murphy, D. M., Nault, B. A., Ray, E. A., Weinzierl, B., Wilson, J. C., Yu, F., Yu, P., Pierce, J. R., and Brock, C. A.: A large source of cloud condensation nuclei from new particle formation in the tropics, Nature, 574, 399–403, https://doi.org/10.1038/s41586-019-1638-9, https://doi.org/10.1038/s41586-019-1638-9, 2019.

Yáñez-Serrano, A. M., Bourtsoukidis, E., Alves, E. G., Bauwens, M., Stavrakou, T., Llusià, J., Filella, I., Guenther, A., Williams, J., Artaxo, P., Sindelarova, K., Doubalova, J., Kesselmeier, J., and Peñuelas, J.: Amazonian biogenic volatile organic compounds under global change, Global Change Biology, 26, 4722–4751, https://doi.org/https://doi.org/10.1111/gcb.15185, https://onlinelibrary.wiley.com/doi/abs/10.1111/gcb.15185, 2020.

Zhao, B., Shrivastava, M., Donahue, N. M., Gordon, H., Schervish, M., Shilling, J. E., Zaveri, R. A., Wang, J., Andreae, M. O., Zhao, C., Gaudet, B., Liu, Y., Fan, J., and Fast, J. D.: High concentration of ultrafine particles in the Amazon free troposphere produced by organic new particle formation, Proceedings of the National Academy of Sciences, 117, 25 344–25 351, https://doi.org/10.1073/pnas.2006716117, https://www.pnas.org/content/117/41/25344, 2020.